SYNAPTIC INPUT TO CHEMICALLY IDENTIFIED BASAL FOREBRAIN NEURONS IN THE RAT

Tibor Hajszán, M.D.

Ph.D. Thesis

Laboratory of Molecular Neurobiology
Institute of Biophysics
Biological Research Center
Hungarian Academy of Sciences

2003

PUBLICATIONS

I. **Hajszán T,** Zaborszky L, Direct Catecholaminergic-Cholinergic Interactions in the Basal Forebrain. III. Adrenergic Innervation of Choline Acetyltransferase-Containing Neurons in the Rat. *J Comp Neurol, 449(2):141-157, 2002. Impact factor: 3.848; times cited: 2*

II. Wu M, **Hajszan T,** Leranth C, Alreja M, Nicotine Recruits a Local Glutamatergic Circuit to Excite Septohippocampal GABAergic Neurons. *Eur J Neurosci, 18:1155-1168, 2003. Impact factor: 4.163*

III. **Hajszan T,** Alreja M, Leranth C, Intrinsic Vesicular Glutamate Transporter 2-Immunoreactive Input to Septo-hippocampal Parvalbumin-Containing Neurons: Novel Glutamatergic Local Circuit Cells. *Hippocampus, in press, 2003. Impact factor: 3.421*

INTRODUCTION

The basal forebrain corticopetal system

Since the classic experiments of Guiseppi Moruzzi and Horace Magoun in the late 1940's (Moruzzi and Magoun, 1949), it has been well known that both sleep and wakefulness are actively induced, actively maintained, and highly organized states of the brain. An extensive network of neurons that is designated as the ascending arousal system (AAS) orchestrates the characteristic forebrain activities during sleep and wakefulness (for review see Rechtschaffen and Siegel, 2000; Hobson and Pace-Schott, 2002; Pace-Schott and Hobson, 2002). In addition to being the effector in the sleep/wake-inducing circuitry, the AAS plays a crucial role in regulating consciousness, cognitive and visceral functions, as well as motor responses by means of controlling the responsiveness of cortical and thalamic neurons to incoming stimuli. The AAS comprises of several widely distributed groups of neurons that can be characterized by their neurotransmitter content (**Fig. 1**). They include the monoaminergic and cholinergic neurons in the brainstem and hypothalamus, the perifornical orexin-containing cells, the cholinergic and GABAergic neurons in the basal forebrain (BF), as well as the glutamatergic neurons in the thalamic intralaminar nuclei (for review see e.g. Saper, 2000; Sutcliffe and de Lecea, 2002).

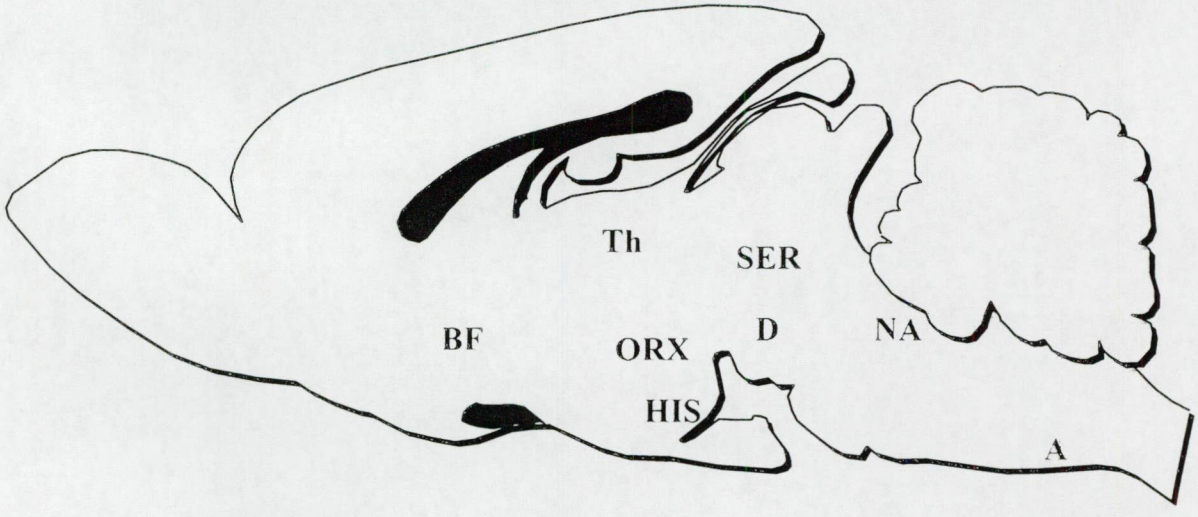

Fig.1. The members of the ascending arousal system. A: central adrenergic system; BF: basal forebrain corticopetal system; D: A8-A1 dopaminergic cell groups; HIS: tuberomammillary histaminergic neurons; NA: locus ceruleus noradrenergic cell group; ORX: posterior hypothalamic orexin-containing neurons; SER: raphe serotonergic system; Th: thalamic intralaminar glutamatergic cells.

The basal forebrain corticopetal system plays a prominent role in the AAS. Since the discovery in the late '70s that Alzheimer's disease is characterized by a severe decline of cholinergic activity in the forebrain (e.g. Dringenberg, 2000), the BF cholinergic system has been in the center of scientific attention. It has also become widely accepted that besides Alzheimer's disease (Muir, 1997), the derailment of the BF cholinergic system can play a role in the pathomechanism of other neurodegenerative and neuropsychiatric disorders such as Parkinson's disease (Jellinger, 1990), or schizophrenia (Sarter and Bruno, 1999). During the past decades, several studies have provided evidence that BF neurons are implicated in the regulation of sleep/wakefulness, sensory processing, attention, learning and memory, and motivation (Everitt and Robbins, 1997; Sarter and Bruno, 2000). The rat cholinergic BF comprises several territories closely associated to the medial and basal surfaces of the cerebral hemispheres (for review see Detari et al., 1999; Jones and Muhlethaler, 1999; Zaborszky et al., 1999; Zaborszky and Duque, 2003). These areas include the medial septum, vertical and horizontal limbs of the diagonal band of Broca, substantia innominata, bed nucleus of stria terminalis (BST), as well as the pallidal regions including the globus pallidus and ventral pallidum. These areas are richly populated by cholinergic, GABAergic, and peptidergic neurons (Zaborszky et al., 1999) that are intermingled with fiber bundles of several ascending and descending neuronal pathways. BF neurons serve either as projection cells innervating the entire cortical mantle, the amygdala, and hippocampus, and/or interneurons forming the complicated circuits underlying local information processing (Zaborszky and Duque, 2000).

Recent discoveries in neuroscience research have raised new important functional and morphological aspects of the basal forebrain corticopetal system. These new discoveries prompted the series of experiments that are detailed in the present thesis. Using neuroanatomical examination techniques, our goal was to address the following specific issues. (1) There is accumulating evidence that the BF cholinergic system participates in autonomic regulation, especially in cardiovascular control (Berntson et al., 1998; Takahashi et al., 2001). It is still unresolved, however, how the viscerosensory information is conveyed to the BF, and how BF cholinergic neurons may affect autonomic regulation. (2) The recently discovered vesicular glutamate transporter (VGLUT) molecules (Aihara et al., 2000; Bellocchio et al., 2000; Takamori et al., 2000) have been proven to be highly specific markers for neurons that utilize glutamate as neurotransmitter. In situ hybridization and

immunohistochemical demonstration of VGLUTs enabled scientists to study the extensive glutamatergic circuitry in the central nervous system. It is well known that glutamate elicits strong functional responses in BF neurons. However, due to the lack of specific methods to visualize glutamatergic neuronal structures, the details of the BF glutamatergic circuitry are still unresolved.

Do basal forebrain cholinergic neurons receive autonomic input?

Based on previous evidence that BF neurons participate in autonomic regulation, we hypothesized that these cells receive neuronal input from known autonomic centers of the brain. To test the validity of our hypothesis, we studied the morphological aspects of a possible adrenergic/cholinergic link in the BF. Previous studies have described significant input to BF neurons from brainstem noradrenergic and serotonergic neurons both in rat (Milner, 1991; Gaykema and Zaborszky, 1996; Zaborszky and Cullinan, 1996; Rodrigo et al., 1998; Leranth and Vertes, 1999) and primates (Smiley and Mesulam, 1999; Smiley et al., 1999). However, these cell groups are well-established members of the AAS in addition to being part of the autonomic network. Thus, the nature of noradrenergic and serotonergic input to the BF cannot be clearly classified as autonomic. On the other hand, the central adrenergic system participates almost exclusively in autonomic and/or neuroendocrine regulation (for review see e.g. Saper, 1995). Therefore, the possible adrenergic innervation of BF cholinergic neurons may transmit only autonomic information.

The neurons that belong to the central adrenergic system are dispersed in the brainstem reticular formation and are arranged in three loose cell groups designated as C1, C2 and C3 (Hökfelt et al., 1974; Armstrong et al., 1982; Hökfelt et al., 1984; Ruggiero et al., 1985). The C1 and C2 groups are frequently characterized as rostral extensions of the A1 and A2 noradrenergic nuclei in the ventrolateral medulla and in the nucleus of the solitary tract, respectively. The cells of the C3 group are distributed along the fibers of the medial longitudinal fascicle, largely corresponding to the area of the nucleus prepositus hypoglossy in the dorsomedial medulla. Adrenergic axons innervate the intermediolateral column of the spinal cord (Tucker et al., 1987; Carlton et al., 1991) and provide viscerosensory information to several brainstem as well as limbic autonomic centers (Saper, 1995).

Earlier biochemical studies (Palkovits and Brownstein, 1988) have provided evidence that both adrenaline and its biosynthetic enzyme, phenylethanolamine N-methyltransferase (PNMT), are undetectable in the majority of BF areas. Even in territories such as the septum, the horizontal limb of the diagonal band (HDB), and BST, where adrenaline and PNMT were detected, the concentration of adrenaline did not exceed 10% of that of noradrenaline. Despite these biochemical data, morphological studies have repeatedly highlighted the widespread existence of PNMT-containing fibers in BF areas both at light and electron microscopic levels (Chang and Kuo, 1989; Phelix et al., 1992; Rodrigo et al., 1998). Tract-tracing experiments have suggested that the adrenergic input to BF originates in the C1-C2 adrenergic cell groups of the brainstem (Semba et al., 1988; Zagon et al., 1994). Nevertheless, morphological studies have concluded that the vast majority of catecholaminergic fibers that innervate BF areas contain dopamine and/or noradrenaline. Along these lines, electrophysiological and pharmacological experiments have primarily studied the effects of dopamine (Momiyama and Sim, 1996) and noradrenaline (Fort et al., 1995) on BF neurons. As a result, it is still unresolved whether the central adrenergic system has any direct physiological influence on the BF. To address the morphological aspect of this issue, we performed a series of light and electron microscopic double-immunolabeling studies in our first set of experiments.

What is the morphological foundation of glutamatergic effect on memory?

The caudal portion of the BF corticopetal system, the medial septum diagonal band complex (MSDB) is known to be involved in the generation of hippocampal theta rhythm and plays a key role in memory and cognitive functions (for review see e.g. Vertes and Kocsis, 1997). The MSDB contains a large population of both cholinergic and GABAergic neurons that project to the hippocampus and/or serve as locally acting interneurons (Jakab and Leranth, 1994). Since the discovery that cholinergic neurons of the MSDB undergo severe atrophy in various neurodegenerative disorders, such as Alzheimer's and Parkinson's disease (Whitehouse et al., 1982; Mufson et al., 1989; Arendt et al., 1995), the septo-hippocampal cholinergic pathway has become one of the well characterized systems of the brain. In contrast to these septo-hippocampal cholinergic neurons that innervate a broad range of hippocampal cells (Frotscher and Leranth, 1985), the GABAergic neurons of the septo-hippocampal pathway (Kohler et al., 1984) selectively inhibit specific populations of GABA

cells in the hippocampus (Freund and Antal, 1988). Via this connection, the septo-hippocampal GABA neurons exert a powerful disinhibitory influence on hippocampal pyramidal cells. Several studies have suggested that tonic impulse flow in this septo-hippocampal GABAergic pathway may be critical for the generation of theta rhythm and normal cognitive functions (Lee et al., 1994; Alreja et al., 2000; Wu et al., 2000).

During the past decade, several authors have reported that intraseptal perfusion of glutamatergic drugs is able to powerfully influence the hippocampal theta rhythm and memory processes (Izquierdo, 1994; Puma and Bizot, 1999; Carre and Harley, 2000) supposedly by controlling the activity of septo-hippocampal neurons. Several studies have suggested that the sources of glutamatergic input to the MSDB may be in the frontal cortex (Jaskiw et al., 1991), entorhinal cortex (Leranth et al., 1999), supramammillary area (Leranth and Kiss, 1996; Kiss et al., 2000), and nucleus reuniens thalami (Bokor et al., 2002). Based on these data, we hypothesized that glutamatergic axons innervate septo-hippocampal GABAergic cells. Since the presence of glutamatergic neurons has been strongly suggested in septal areas (Gonzalo-Ruiz and Morte, 2000; Manns et al., 2001; Kiss et al., 2002), we also speculated that the source of the glutamatergic innervation is, at least in part, intrinsic to the septum. Since the septal glutamatergic cell bodies and the putative local targets of their terminals occupy the same and/or closely associated areas, tracing these glutamatergic local circuit neurons with retrograde tracers injected into the MSDB would produce questionable results. Therefore, to clarify whether the glutamatergic input to the MSDB comes from local sources and/or from extraseptal origin, we surgically separated the septum from part of its afferents by septal undercut and fimbria/fornix transection in our second set of experiments. Subsequently, simultaneous immunohistochemical visualization of the recently discovered specific glutamatergic marker VGLUTs (Aihara et al., 2000; Bellocchio et al., 2000; Takamori et al., 2000) and parvalbumin enabled us to test the validity of our hypotheses.

MATERIALS AND METHODS

Animals and surgical procedures

Animals. Adult male Sprague-Dawley rats (250-300 g; Charles River, Wilmington, MA) were group-housed and maintained on a 12/12 h light/dark cycle and provided with unlimited access to water and rat chow. All animal protocols used in this study were in compliance with the National Institutes of Health Guide for the Care and Use of Laboratory Animals. All surgical interventions and perfusions were carried out using a ketamine-based anesthetic [ketamine (25 mg/ml), xylazine (1.2 mg/ml), and acepromazine (0.03 mg/ml) in saline; 3 ml/kg, i.m.].

Septal undercut (SX). In order to isolate the MSDB from all of its ventral afferents coming from the right side, unilateral septal undercut was carried out according to our standard protocol (Szeidemann et al., 1995). Briefly, rats (n=6) were fixed into a stereotaxic apparatus (David Kopf Instruments, Tujunga, CA) and an L-shaped knife with the tip facing towards the nose was sunken into the right lateral ventricle at the rostral end of the septum in a position parallel to the sagittal plane (stereotaxic coordinates: AP: 1.60; L: 1.50; V: 8.00). The knife was then rotated by 90° towards the sagittal plane and pulled back up to the caudal end of the septum (AP: 0.26). Finally, the knife was rotated back to its original position and removed. Rats were allowed to survive for five or ten days after SX. Following fixation and Vibratome sectioning, all lesion sites were examined throughout their rostro-caudal extent. Only brains with complete lesions extending from the lateral ventricle to the basal surface of the MSDB (**Fig. 11a**) were used in the experiments.

Fimbria/fornix transection (FFX) was done according to our standard protocol (Leranth et al., 2000) to separate the MSDB from all afferents coming from the hippocampus via the right fimbria/fornix. Briefly, rats (n=6) were fixed into a stereotaxic apparatus and from a dorsal penetration, the overlying cortical areas and corpus callosum were aspirated. Then, under clear visual control, the right fimbria/fornix was completely disrupted by vacuum aspiration. Following surgery, the rats were allowed to survive for five or ten days.

Colchicine treatment. In order to visualize VGLUT2-immunoreactive (IR) cell bodies in the septum, the axonal-transport blocker, colchicine was applied to enhance the accumulation of VGLUT2 in the perikarya. Under stereotaxic control, rats (n=3) were

injected with 180 μg colchicine [dissolved in 20 μl 0.1 M phosphate-buffered saline (PBS; pH=7.60)] into the lateral ventricle using a Hamilton microsyringe (stereotaxic coordinates: AP: 0.90; L: 1.50; V: 4.00). Following the colchicine injection, rats were allowed to survive for 40 hours.

Tissue processing for light microscopy

Rats were transcardially perfused with 50 ml PBS, then either by a 100 ml mixture of 4% acrolein and 2% paraformaldehyde and, subsequently, 200 ml 2% paraformaldehyde (experiment I; n=6) or by 400 ml fixative containing 4% paraformaldehyde, 0.1% glutaraldehyde and 15% picric acid (experiment II) in PBS. The brains were removed and postfixed overnight in 4% paraformaldehyde dissolved in PBS. Coronal Vibratome sections (50 μm) were cut into either six series from the BF (experiment I) or four separate sets throughout the MSDB (experiment II) and collected in PBS. Different sets of sections from each brain were used for light and electron microscopic processing. For light microscopy, the tissue was immunostained as described below, then the sections were mounted on gelatin-coated slides, air-dried, cleared in xylenes, coverslipped with Permount and analyzed under an Olympus BX60 microscope (Olympus Optical, Tokyo, Japan) equipped with a Zeiss AxioCam digital camera.

Immunohistochemical procedures

Experiment I. In order to visualize adrenergic and cholinergic neuronal structures, PNMT and choline acetyltransferase (ChAT), the synthesizing enzymes for adrenaline and acetylcholine, respectively, were detected as markers. All incubations detailed below were done at room temperature (RT) unless otherwise specified. For simultaneous immunoperoxidase labeling of PNMT and ChAT, the tissue was incubated overnight in a mixture of polyclonal rabbit anti-PNMT [1:10,000; (Bohn et al., 1987)] and polyclonal sheep anti-ChAT (1:20,000; Chemicon, Temecula, CA) diluted in PBS containing 2% normal horse serum and 0.5% triton. After rinsing in PBS, the sections were incubated in biotinylated goat anti-rabbit IgG (Vector Laboratories, Burlingame, CA; 1:500 in PBS containing 2% normal horse serum and 0.5% triton; overnight) followed by ABC Elite (Vector Laboratories; 1:500 in PBS; 2 hours). Following a brief rinse in TRIS-buffered saline (TBS; pH=7.60), PNMT-IR

elements were visualized using a nickel-diaminobenzidine chromogen (0.4 mg/ml 3,3'-diaminobenzidine tetrahydrochloride, 0.4 mg/ml nickel ammonium sulfate and 0.0006% hydrogen peroxide dissolved in TBS). This reaction resulted in the black staining of PNMT-IR elements. The nickel-diaminobenzidine precipitate was silver-gold intensified as described earlier (Liposits et al., 1984), but the thyoglycolic acid pretreatment was omitted from the protocol. The ChAT-IR neuronal structures were visualized by incubating the sections, already immunostained for PNMT, in biotinylated donkey anti-sheep IgG (Jackson ImmunoResearch Laboratories, West Grove, PA; 1:500 in PBS containing 2% normal horse serum and 0.5% triton; overnight) and then in ABC Elite. The tissue went through the biotin-tyramide amplification procedure followed by the peroxidase reaction using the diaminobenzidine chromogen (0.4 mg/ml 3,3'-diaminobenzidine tetrahydrochloride and 0.0006% hydrogen peroxide dissolved in TBS) that resulted in light brown staining of ChAT-IR neurons.

Experiment II. In order to visualize glutamatergic and septo-hippocampal GABAergic neuronal structures, VGLUT1 and VGLUT2 were detected as markers for glutamatergic elements and parvalbumin for the septo-hippocampal GABAergic neurons (Freund, 1989). The immunostaining was carried out as described above using polyclonal guinea pig anti-VGLUT1 (1:20,000; Chemicon), polyclonal guinea pig anti-VGLUT2 (1:20,000; Chemicon), and monoclonal mouse anti-parvalbumin (1:1000; Sigma, Saint Louis, MO). The applied secondary antibodies were biotinylated donkey anti-guinea pig IgG (1:500; Jackson ImmunoResearch Laboratories) for VGLUT1 and VGLUT2 and biotinylated horse anti-mouse IgG (1:500; Vector Laboratories) for parvalbumin. VGLUT- and parvalbumin-IR elements were visualized using the nickel-diaminobenzidine and diaminobenzidine chromogens, respectively.

Control. As a control for immunostaining, some sections were immunostained as described above, but the primary antisera were replaced with non-immune serum. No immunostaining or cross-reaction was registered in these control experiments.

Tissue processing for electron microscopy

Sections were double-immunostained for PNMT/ChAT and VGLUT2/parvalbumin as described above, although the preservation of ultrastructural details required the complete

omission of triton from all solutions. Instead, to enhance antibody penetration, the sections were incubated in a cryoprotective solution (25% sucrose, 10% glycerol in 0.01 M PBS; 2 hours) and freeze-thawed in liquid nitrogen prior to incubation in the primary antibodies. After the immunohistochemical procedure, the sections were osmicated (1% osmium tetroxide in PBS; 40 min), dehydrated in ethanol (the 70% ethanol contained 1% uranyl acetate; 40 min) and flat embedded in Araldite (Electron Microscopy Sciences, Fort Washington, PA) between liquid release agent-coated slides and coverslips. Putative synaptic contacts were selected under the light microscope. The selection criteria are described in detail below in the quantitative analysis section. The selected structures were photo-documented and reembedded in Araldite blocks. Serial ultrathin sections were cut and collected on single-slot Formvar-coated grids and examined in a Tecnai 12 transmission electron microscope equipped with an AMT Advantage 4.00 HR/HR-B CCD camera system (Advanced Microscopy Techniques, Danvers, MA).

Quantitative analysis and digital imaging

All quantitative analyses were performed from groups of three successfully treated animals. In statistical analyses, data were summarized and diagrams were constructed using the Microsoft Excel 97 software. Significance of changes was determined with the Student's t-test. Contrast and lightness were adjusted on digital images, and figures were assembled and lettering was added using the Adobe PhotoShop 6.0 software. The figures were printed with an Epson Stylus Photo 700 printer.

Mapping and quantitative analysis of adrenergic/cholinergic interactions in the BF. For the mapping and quantitative analysis of putative contact sites between adrenergic boutons and cholinergic neuronal profiles, a computer-controlled Zeiss Axioskop microscope equipped with the Neurolucida software (MicroBrightField, Colchester, VT) was used. Screening with the 100x oil-immersion lens, ChAT-IR cell bodies and adrenergic/cholinergic appositions were mapped in sections from six different rostro-caudal levels of a representative brain. For quantitative analysis, numbers of cholinergic perikarya and adrenergic/cholinergic appositions were obtained from maps of sections from three brains at three different rostro-caudal levels of the BF. Appositions were mapped and counted only if they qualified for electron microscopic analysis, i.e. side-to-side contacts with both the adrenergic bouton and

the cholinergic profile strictly in the same focal plane with no discernible gap between the structures. Profiles mapped and counted as cholinergic cell bodies were ChAT-IR perikarya with clearly recognizable cell nucleus.

In order to find out whether there are any statistical differences in the distribution patterns of adrenergic/cholinergic appositions across BF territories, statistical analysis was used based on data obtained from the Neurolucida mappings. A hypothetical distribution pattern of adrenergic/cholinergic appositions was established based on the null hypothesis that the appositions are distributed homogeneously on BF cholinergic neurons across the entire extent of the BF. To construct this hypothetical pattern, a ratio of PNMT/ChAT appositions per cholinergic cell body was computed by dividing the total number of appositions by the total number of ChAT-IR cell bodies for each brain. The numbers of cholinergic neurons in individual BF areas were then multiplied with this ratio to arrive at the hypothetical amount of appositions in case of homogeneous distribution. The Student's t-test was finally used to determine whether there are any significant differences between the hypothetical homogeneous and the actual distribution patterns.

VGLUT2 bouton density analysis in the MSDB. In order to quantitatively analyze the relative changes in VGLUT2 bouton density caused by the deafferentations, sections from intact, SX, and FFX animals (three rats in each group) were immunolabeled for VGLUT2 as described above. Thereafter, high power (100x objective lens) non-overlapping light micrographs were taken at three different rostro-caudal levels [rostral: Bregma +0.80; middle: Bregma +0.40; caudal: at Bregma] from septal areas, such as the medial septum/lateral septum border zone (MS/LS) both ipsi- and contralateral to the lesion, and from the middle septal area (between the right and left MS/LS, along the midline). VGLUT2-immunopositive varicosities were counted within 400 μm^2 unit areas that were randomly selected from each micrograph by blind dropping an overlay grid onto the printed pictures. Only those varicosities were considered that were clearly in focus. Bouton densities obtained this way were statistically compared between ipsi- and contralateral MS/LS in SX and FFX animals, as well as between the same areas of SX versus intact and FFX versus intact rats.

Quantitative analysis of VGLUT2 input to parvalbumin-positive neurons in the MSDB. To reveal whether SX has any influence on the VGLUT2 innervation of MSDB parvalbumin neurons, sections from intact and SX animals (three rats in each group) were

double-immunostained for VGLUT2 and parvalbumin as described above. Then, by high magnification light microscopic screening of both sides of the MSDB at the three different rostro-caudal levels specified above, parvalbumin cells were counted and sorted into two groups. Parvalbumin neurons were sorted into the first group if they were contacted by VGLUT2 boutons according to the following criteria: Parvalbumin cells were considered as targets of VGLUT2-IR boutons, if at least one VGLUT2 varicosity was found in close apposition either to the cell body or to a dendrite being continuous with the perikaryon. Parvalbumin cells that did not fulfill these criteria were sorted into the second group. These very same criteria were applied for both the electron microscopic studies and the quantitative analysis. Thus, the validity of the light microscopic quantitative analysis of VGLUT2 input to parvalbumin-positive neurons is backed by the ultrastructural findings. Finally, the amount of parvalbumin neurons contacted by VGLUT2 boutons (first group) was expressed as the percentage of all parvalbumin cells in the MSDB (first group + second group). These data obtained from SX animals were then statistically compared to those from intact rats. FFX animals were not analyzed in this way because similar to a previous study (Peterson et al., 1987), we observed a severe loss of parvalbumin-IR cells in the MSDB following FFX.

RESULTS

Experiment I

Distribution of PNMT-positive fibers/terminals in relation to cholinergic neurons

Medial septum diagonal band complex. In the dorsal part of the septal complex, a PNMT-positive fiber network was found to occupy a position laterodorsal to the bulk of cholinergic cell bodies (**Fig. 2a**). However, some scattered adrenergic axons were observed as they approached ChAT-positive profiles along the lateral border of the medial septum. Around the ventral part of the vertical limb of the diagonal band (VDB) where it bends into the HDB, an especially rich network of PNMT-IR fibers was visible. In this region, a few adrenergic varicosities appeared to be closely associated with cholinergic profiles (**Fig. 2b**).

Horizontal limb of the diagonal band of Broca. PNMT-containing fibers were found to accumulate along the borders of HDB, running mediolaterally close to the basal surface of the brain and adjacent to the ventral pallidum and substantia innominata (**Fig. 2c**). Adrenergic axons in the medial part of HDB appeared to originate from a rich network around the organum vasculosum of the lamina terminalis and pass underneath the ventral part of the VDB (**Fig. 2b**). From the borders, the mediolaterally-running PNMT-positive axons gave rise to perpendicular side branches (**Fig. 2c**) that approached neighboring cholinergic neurons (**Fig. 2d-f**). Caudally, close to the ventromedial border of the HDB, cholinergic neurons closely associated with the hypothalamic supraoptic nucleus (SON) were embedded in a relatively rich network of adrenergic axons (**Fig. 2g**).

Ventral pallidum. In the ventral pallidum (not shown), both PNMT-positive fibers and cholinergic structures were scarce. However, sparse to moderate amounts of adrenergic axons were observed ventromedially along the border to the HDB and dorsomedially near the border to the BST.

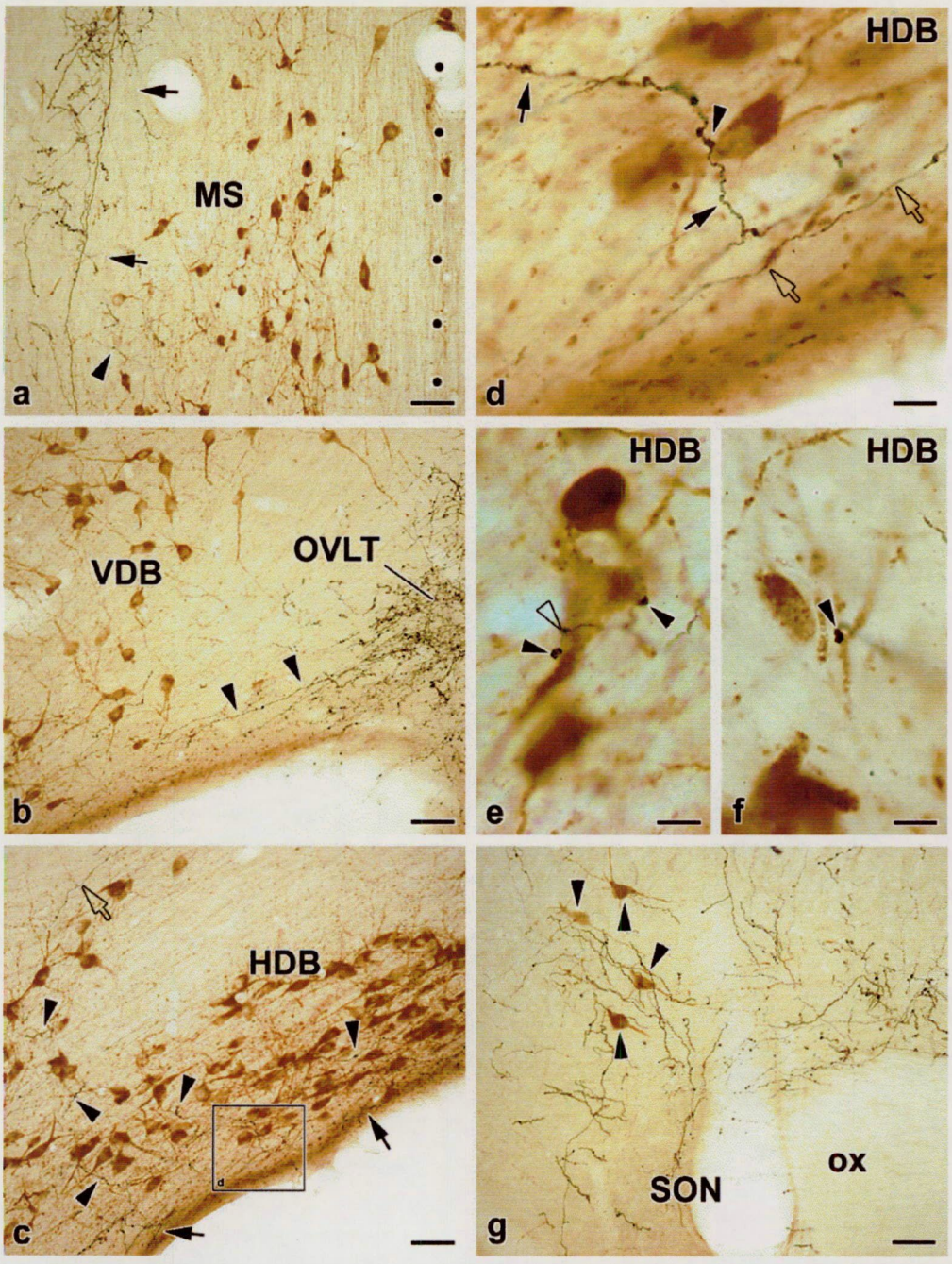

Fig. 2. The low power photomicrographs (a-c), taken from double-immunostained coronal sections of the rat brain, demonstrate the dorsal (a) and ventral (b) parts of the septal complex and the horizontal limb of diagonal band of Broca (HDB, c). The high power micrographs (d-f) demonstrate putative adrenergic/cholinergic interaction sites. a: In the dorsal part of the septal complex, a phenylethanolamine N-methyltransferase (PNMT)-positive fiber network (arrows) occupies a position laterodorsal to the cholinergic cell bodies of the medial septum (MS). Some scattered adrenergic axons (arrowhead) approach choline acetyltransferase (ChAT)-positive profiles. Dots represent the midline. Scale bar: 50 μm. **b:** An especially rich PNMT-positive fiber network is visible in the organum vasculosum of the lamina terminalis (OVLT). Some mediolaterally-running axons seem to emanate from this network (arrowheads) on their course underneath the ventral part of the vertical limb of diagonal band of Broca (VDB) towards the HDB. Scale bar: 50 μm. **c:** Mediolaterally-running PNMT-positive fibers are distributed along both the ventral (solid arrows) and dorsal (open arrow) borders of the HDB. From this network, perpendicular side branches originate (arrowheads) and approach neighboring cholinergic neurons. The territory in the rectangle is enlarged in (**d**). Scale bar: 50 μm. **d-f:** These high power photomicrographs demonstrate representative adrenergic/cholinergic appositions taken from the HDB. In (**d**), both the thick (solid arrows) and thin (open arrows) types of adrenergic axons are visible. The open arrowhead in (**e**) points to a varicosity on a thin-type adrenergic fiber in close apposition to a ChAT-positive profile that is also contacted by thick fibers (solid arrowheads). Scale bars: 10 μm. **g:** Scattered cholinergic neurons (arrowheads) positioned dorsolateral to the hypothalamic supraoptic nucleus (SON) are embedded in a rich PNMT-positive fiber network. ox: optic chiasma. Scale bar: 50 μm.

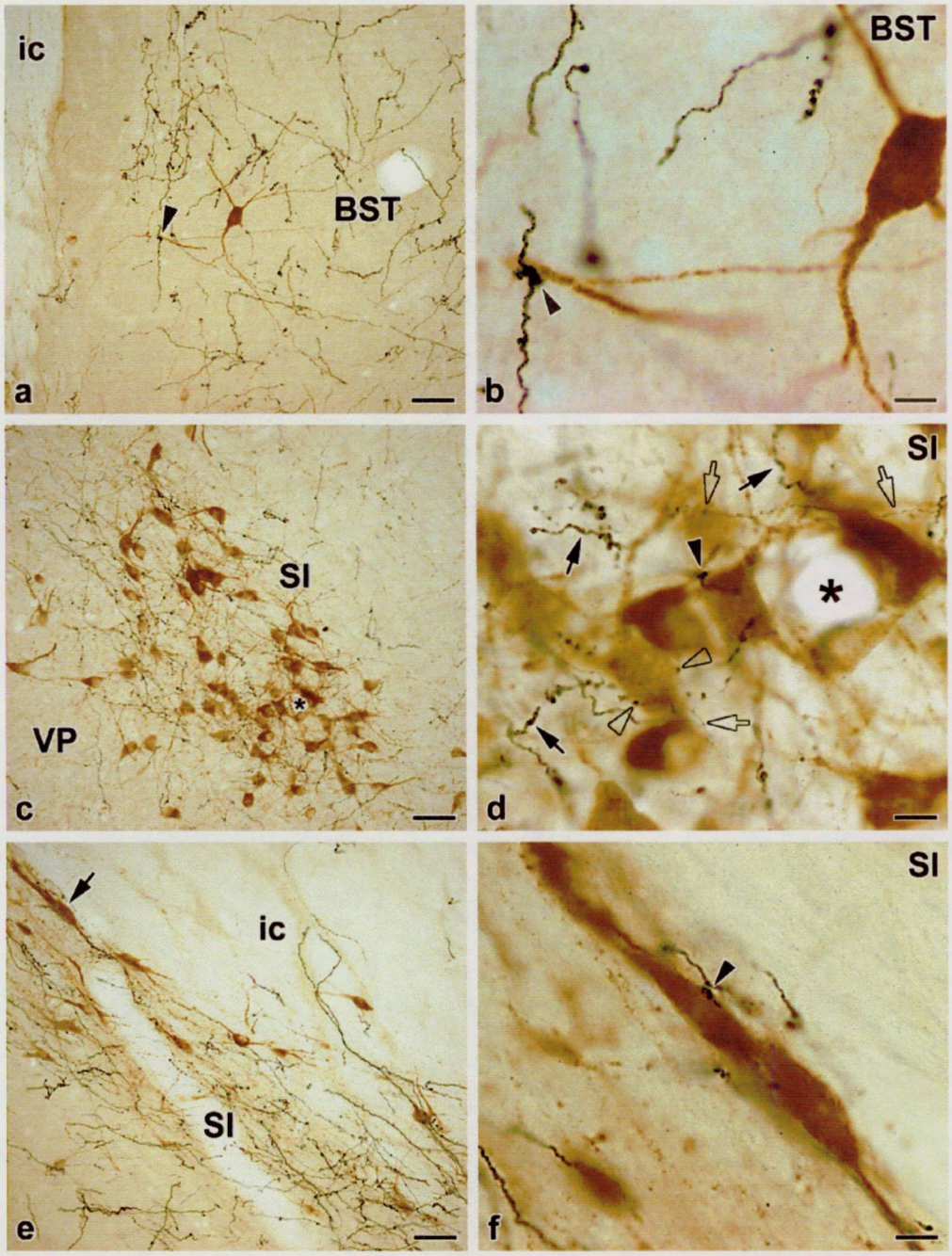

Fig. 3. The low power photomicrographs (a, c, and e), taken from double-immunostained coronal sections of the rat brain, demonstrate the lateral part of the bed nucleus of stria terminalis (BST, a) and the rostral (c) and caudal (e) substantia innominata (SI). The high power micrographs (b, d, and f) are enlargements from their low power counterparts demonstrating adrenergic/cholinergic appositions. a: In the BST, a single cholinergic neuron is embedded in a rich meshwork of phenylethanolamine N-methyltransferase (PNMT)-positive fibers. The arrowhead points to a putative contact that is enlarged in (**b**). ic: internal capsule. Scale bar: 50 μm. **b:** An adrenergic/cholinergic apposition (arrowhead) enlarged from (**a**). Scale bar: 10 μm. **c:** This micrograph demonstrates a part of the rostral SI as indicated by the rectangle in Fig. 4d. A characteristic cluster of cholinergic neurons receives a heavy supply of PNMT-positive fibers. Scale bar: 50 μm. **d:** Enlargement from (**c**). For orientation, the asterisks in both (**c**) and (**d**) label the same vessel. Cholinergic neuronal elements are embedded in a network containing both thick (solid arrows) and thin (open arrows) types of adrenergic axons. Examples of putative contacts established by large (solid arrowhead) and small (open arrowheads) boutons are shown. Scale bar: 10 μm. **e:** In the caudal SI, scattered choline acetyltransferase (ChAT)-positive neurons are surrounded by adrenergic fibers. The solid arrow points to cholinergic neurons that are enlarged in (**f**). Scale bar: 50 μm. **f:** Enlargement from (**e**). A fusiform ChAT-positive cell is contacted by a large adrenergic bouton (arrowhead). Scale bar: 10 μm.

Globus pallidus and internal capsule. The globus pallidus (not shown) contained moderate amounts of PNMT-positive fibers at its ventral and ventromedial borders near the internal capsule. Within the internal capsule (not shown), many adrenergic fibers of passage were observed heading between the BST and the substantia innominata. Occasionally, these axons gave rise to terminal boutons that established close contacts with neighboring cholinergic profiles.

Bed nucleus of stria terminalis. Despite the massive adrenergic innervation of the BST, the adrenergic/cholinergic interaction sites encountered here were very infrequent due to the low number of cholinergic profiles (**Fig. 3a-b**).

Substantia innominata. A rich network of PNMT-IR axons was observed throughout the rostro-caudal extent of the substantia innominata. Within a characteristic area of a cholinergic cell cluster (**Fig. 3c**) as well as in the caudalmost part of the substantia innominata (**Fig. 3e**), both adrenergic fibers and ChAT-IR neurons appeared to accumulate. In these areas, PNMT-positive axons were aligned parallel with and wrapped around bundles of cholinergic dendrites and numerous close associations (**Fig. 3d,f**) were encountered. Although fine adrenergic fibers occasionally climbed around thin ChAT-positive dendrites, the majority of contacts were individual established by en passant boutons as their intervaricose segments crossed over the cholinergic profiles.

Distribution and quantitative analysis of PNMT/ChAT appositions

The schematic drawings of **Figure 4** illustrate the distribution pattern of PNMT-positive varicosities in close apposition to cholinergic profiles at six different rostro-caudal levels of a representative brain. The adrenergic/cholinergic appositions showed an uneven distribution across different BF structures. Preferential distribution sites were in the ventral part of HDB (**Fig. 4a-d**), within the cholinergic cell cluster of the substantia innominata (**Fig. 4d**), and in a narrow band bordering the substantia innominata from the globus pallidus and internal capsule (**Fig. 4e-f**). The majority of appositions were found in the substantia innominata (51%) followed by the HDB (30%). The remaining BF structures together contained 19% of all appositions.

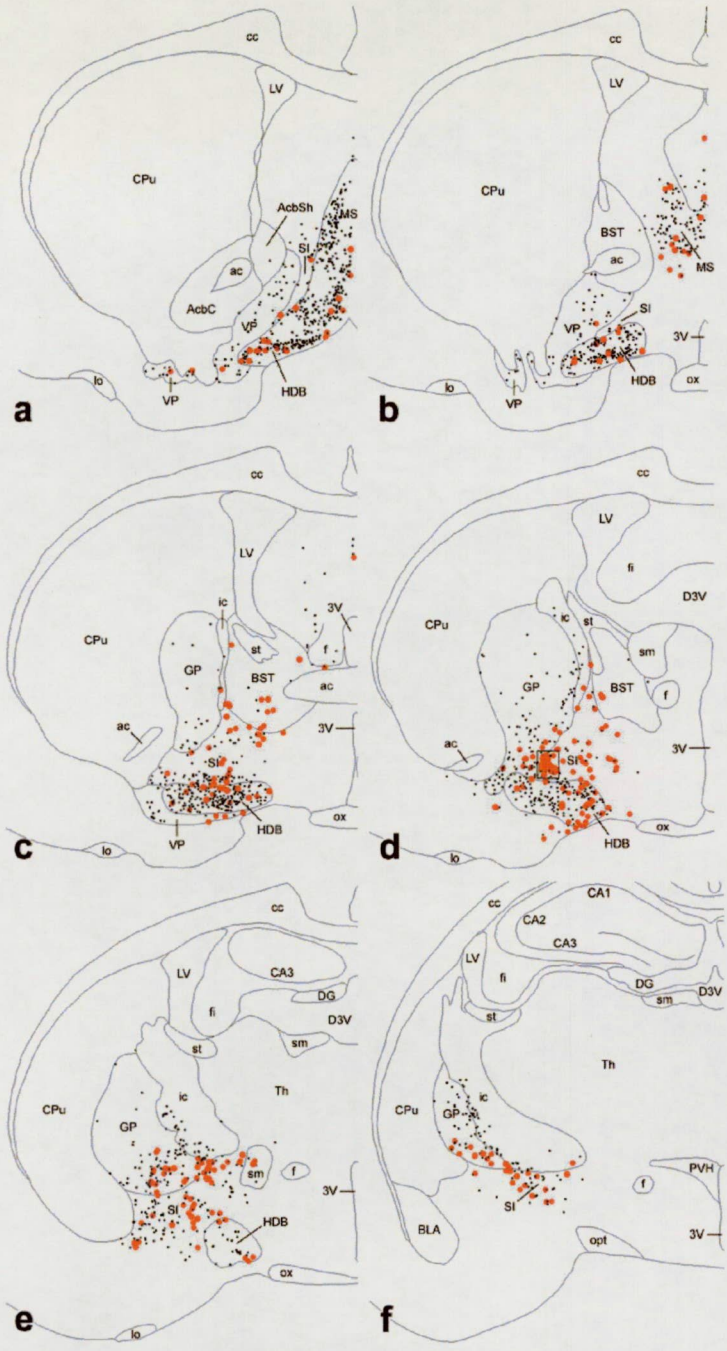

Fig. 4. These schematic drawings illustrate the distribution pattern of phenylethanolamine N-methyltransferase (PNMT)-positive varicosities in close apposition to cholinergic profiles at six different rostro-caudal levels of the rat basal forebrain. Red spots represent adrenergic/cholinergic appositions, while black dots represent cholinergic perikarya. The rectangle in (**d**) indicates the territory demonstrated in the micrograph of **Fig. 3c**. 3V: 3rd ventricle; ac: anterior commissure; AcbC: nucleus accumbens, core; AcbSh: nucleus accumbens, shell; BLA: basolateral amygdaloid nucleus; BST: bed nucleus of stria terminalis; CA1-3: fields CA1-3 of hippocampus; cc: corpus callosum; CPu: caudate putamen; D3V: dorsal 3rd ventricle; DG: dentate gyrus; f: fornix; fi: fimbria of hippocampus; GP: globus pallidus; HDB: horizontal limb of diagonal band of Broca; ic: internal capsule; lo: lateral olfactory tract; LV: lateral ventricle; MS: medial septum; opt: optic tract; ox: optic chiasma; PVH: paraventricular nucleus of hypothalamus; SI: substantia innominata; sm: stria medullaris; st: stria terminalis; Th: thalamus; VP: ventral pallidum.

By comparing a hypothetical homogeneous distribution of PNMT/ChAT appositions with the actual pattern, the analysis (**Fig. 5**) demonstrated that the number of adrenergic appositions was significantly ($p<0.05$) higher in the substantia innominata than it should be in case of homogeneous distribution (an average of 90.3 actual appositions versus 27.5 appositions for homogeneous distribution). On the other hand, the septal complex contained significantly fewer appositions (8.3 versus 38.3) and the significance of this difference was even stronger ($p<0.01$). The numbers of appositions in all of the remaining areas were not significantly different from those of the hypothetical homogeneous distribution.

Ultrastructural characteristics of PNMT/ChAT relations

In our correlated light and electron microscopic studies, diamonibenzidine was used to label cholinergic neurons and the

silver-gold intensified nickel-diaminobenzidine to stain PNMT-positive structures. At the light microscopic level, adrenergic fibers and terminals appeared in black and were easily differentiated from ChAT-positive elements that were revealed by brown deposits of diaminobenzidine. This color difference persisted after osmication and plastic embedding of the sections. Furthermore, the presence of the highly electron-dense silver-gold grains in the PNMT-positive structures made the electron microscopic identification of adrenergic profiles obvious.

A total of 16 individual PNMT-immunoreactive varicosities, closely associated to cholinergic profiles, were randomly selected for ultrastructural analysis. Ten appositions were classified as axodendritic involving either proximal or distal cholinergic dendrites. During the ultrastructural analysis, eight of them were confirmed as synaptic. All of these axodendritic synapses were of the asymmetric type with clear and prominent postsynaptic densities (**Fig. 6**). The remaining 6 selected boutons were located adjacent to cholinergic cell bodies, however only one of them was confirmed as synaptic. **Figure 7** demonstrates that this identified axosomatic synapse is of the symmetric type. In the other cases, the identification of synapses was either precluded by the presence of dense immunoprecipitate at the contact sites or the ultrastructural investigation revealed intervening glial processes between PNMT-positive varicosities and cholinergic profiles. In some cases, adrenergic boutons were observed as they established synaptic contacts with chemically unidentified neuronal profiles in the BF.

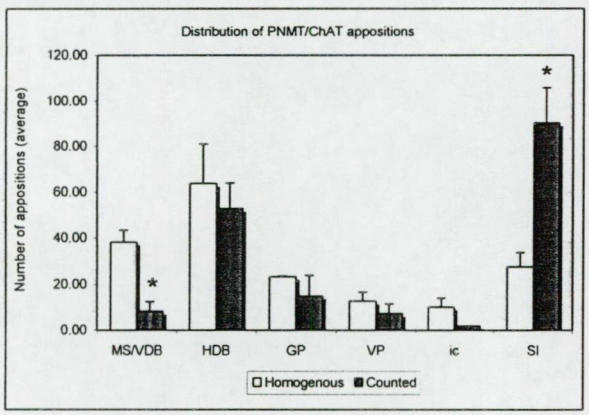

Fig. 5. Quantitative analysis of the distribution of adrenergic/cholinergic appositions in the rat basal forebrain based on data obtained from the Neurolucida mappings (Fig. 4). Open columns represent the null hypothesis as average numbers of appositions in each area, as it would be in case of hypothetical homogeneous distribution, while solid columns show the averages of actual numbers. As indicated by the asterisks, the differences between homogeneous and actual distributions are significant in the septal complex and in the SI. Bars represent standard deviation. ChAT: choline acetyltransferase; GP: globus pallidus; HDB: horizontal limb of diagonal band of Broca; ic: internal capsule; MS/VDB: septal complex; PNMT: phenylethanolamine N-methyltransferase; SI: substantia innominata; VP: ventral pallidum.

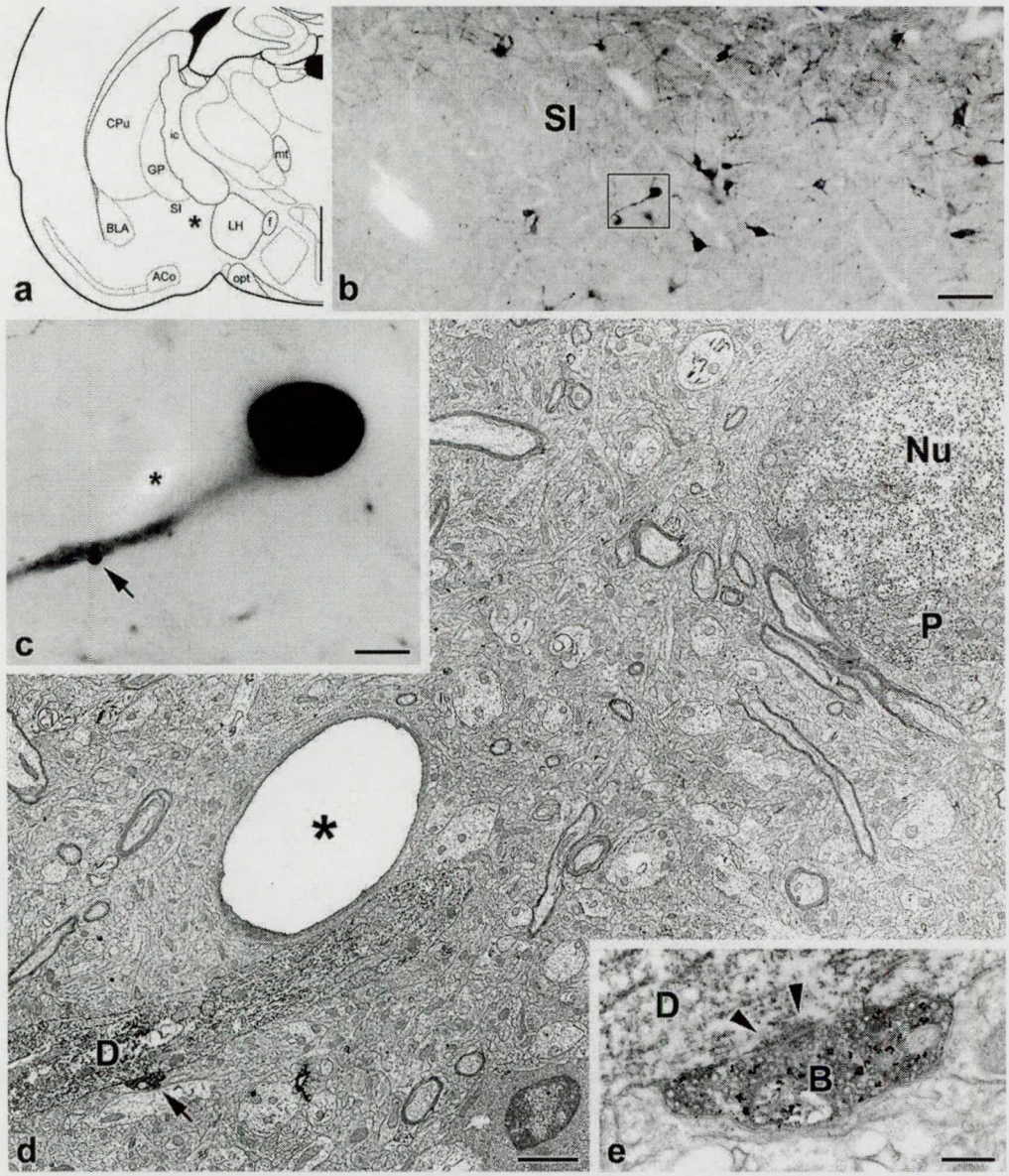

Fig. 6. This composite picture demonstrates the correlated light and electron microscopic analysis of an axodendritic, asymmetric type synapse between an adrenergic bouton and a cholinergic dendrite in the substantia innominata (SI). a: Schematic map of a coronal section of rat brain at the level of the caudal basal forebrain. In the SI, the asterisk indicates the position of the neuronal profiles that were selected for ultrastructural analysis. ACo: anterior cortical amygdaloid nucleus; BLA: basolateral amygdaloid nucleus; CPu: caudate putamen; f: fornix; GP: globus pallidus; ic: internal capsule; LH: lateral hypothalamic area; mt: mamillothalamic tract; opt: optic tract. **b:** This low power photomicrograph, taken from a double-immunostained, resin-embedded coronal section, demonstrates the area labeled by the asterisk in (**a**). The region in the rectangle contains the selected neuronal structures that are enlarged in (**c**). Scale bar: 80 μm. **c:** This high power photomicrograph demonstrates the area indicated by the rectangle in (**b**). The arrow points to a large adrenergic varicosity abutting a proximal dendrite of a cholinergic neuron. Note that the initial segment of the dendrite is out of focus. Scale bar: 8 μm. **d:** Low power electron micrograph correlated to the micrograph of (**c**). For orientation, the asterisks in both (**c**) and (**d**) label the same capillary. The highly electron-dense adrenergic bouton (arrow) is in direct contact with the cholinergic dendrite (D). As predicted by the photomicrograph of (**c**), the initial segment of the dendrite is not visible at this level. Nu: cell nucleus; P: cholinergic perikaryon. Scale bar: 2 μm. **e:** The high power electron micrograph reveals that the adrenergic bouton (B), containing silver-gold grains, forms an asymmetric type synapse (arrowheads) with the cholinergic dendrite (D). Scale bar: 300 nm.

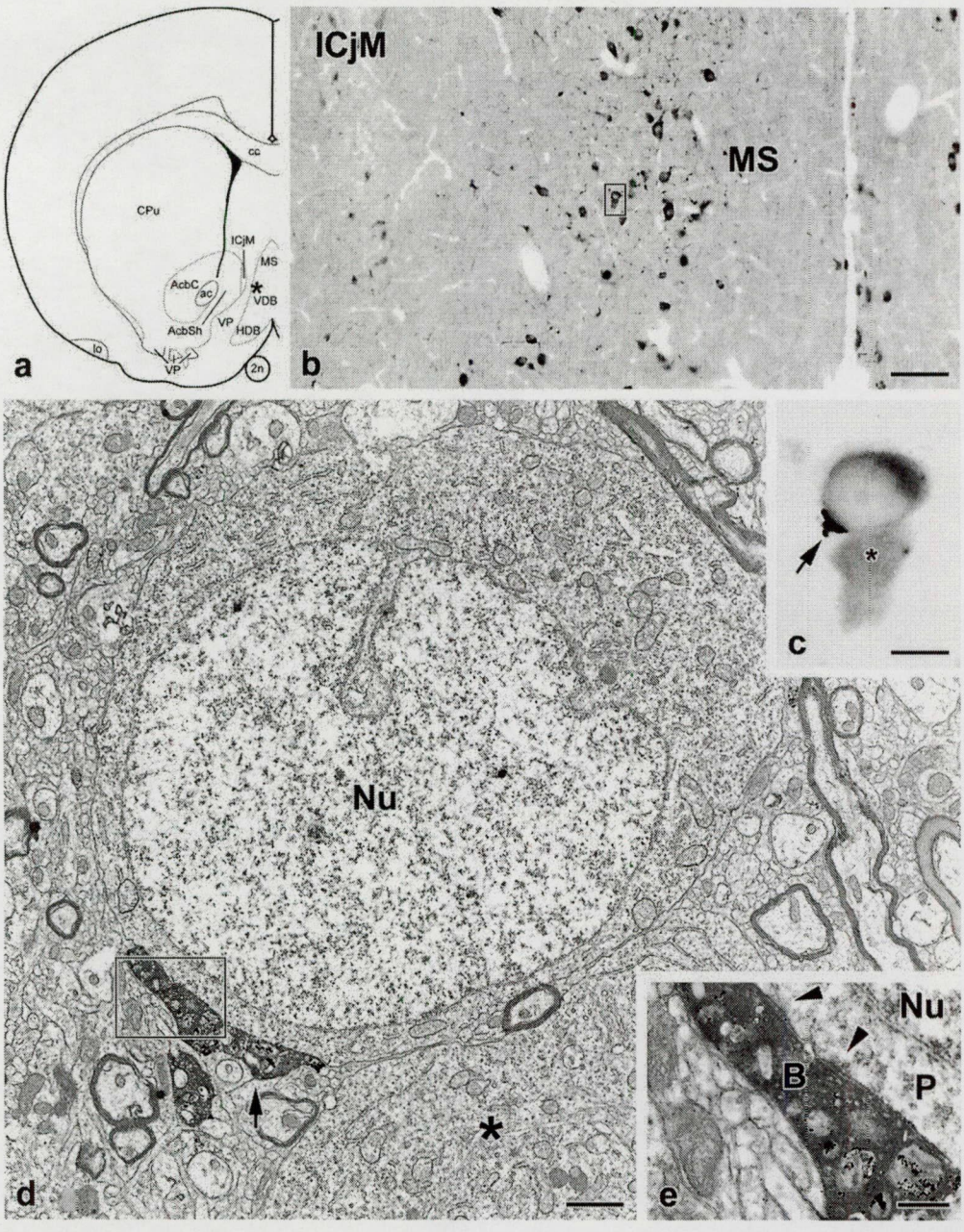

Fig. 7. This composite picture demonstrates the correlated light and electron microscopic analysis of an axosomatic, symmetric type synapse between an adrenergic bouton and a cholinergic cell body in the septal complex. a: Schematic map of a coronal section of rat brain at the level of the rostral basal forebrain. In the septal complex, the asterisk indicates the position of the neuronal profiles that were selected for ultrastructural analysis. 2n: optic nerve; ac: anterior commissure; AcbC: nucleus accumbens, core; AcbSh: nucleus accumbens, shell; cc: corpus callosum; CPu: caudate putamen; HDB: horizontal limb of diagonal band of Broca; ICjM: island of Calleja, major island; lo: lateral olfactory tract; MS: medial septum; VDB: vertical limb of diagonal band of Broca; VP: ventral pallidum. **b:** The low power photomicrograph, taken from a double-immunostained, plastic-embedded coronal section of the rat brain, demonstrates the area labeled by the asterisk in (**a**). The rectangle highlights the selected neuronal structures that are enlarged in (**c**). Scale bar: 80 μm. **c:** This high power photomicrograph demonstrates the area indicated by the rectangle in (**b**). The arrow points to a large adrenergic varicosity in close proximity to a cholinergic perikaryon. Scale bar: 8 μm. **d:** Low power electron micrograph correlated to the micrograph of (**c**). For orientation, the asterisks in both (**c**) and (**d**) label the same neighboring cholinergic cell body. The highly electron dense adrenergic varicosity (arrow) is in direct contact with the cholinergic cell body identified by the diaminobenzidine (DAB) precipitate. The area in the rectangle is enlarged at high power in (**e**). Nu: cell nucleus. Scale bar: 1 μm. **e:** The adrenergic bouton (B), containing both the electron-dense, homogeneous nickel-DAB precipitate and the highly electron-dense silver-gold deposits, establishes symmetric type synaptic contact (arrowheads) with the cholinergic perikaryon (P). Scale bar: 300 nm.

Experiment II

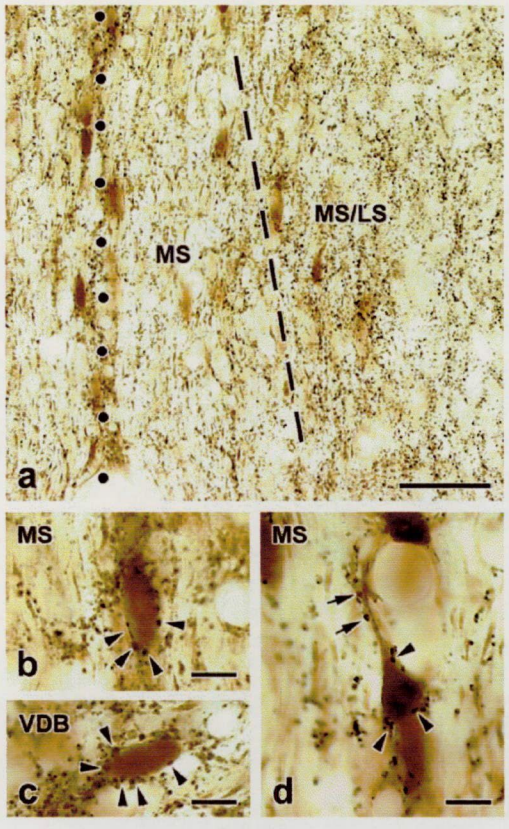

Fig. 8. Vesicular glutamate transporter 2 (VGLUT2)-immunoreactive terminals can be visualized in the vicinity of parvalbumin (PV)-positive neurons within the septal complex. a: Low power light micrograph that shows the distribution of the black VGLUT2-immunopositive varicosities and the brown-colored PV-immunoreactive neuronal structures in the medial septum (MS). Along the midline (marked by dots) where most of the PV neurons reside, relatively few VGLUT2-containing boutons can be observed. VGLUT2-positive varicosities occupy mainly the medial septum/lateral septum border zone (MS/LS, lateral to the dashed line). Scale bar: 50 μm. **b, c, d:** High power light micrographs that demonstrate PV-containing cell bodies from the MS and the vertical diagonal band (VDB) that are surrounded by VGLUT2-immunopositive varicosities and several axosomatic (arrowheads) and axodendritic (arrows) close associations can be seen. Scale bars: 10 μm.

<u>VGLUT2-immunoreactive boutons synapse with parvalbumin-containing neurons in the MSDB</u>

Although the immunostaining of VGLUT1 fibers revealed a rich network of varicosities within the lateral septal areas of intact animals, the MSDB appeared to be almost completely devoid of these boutons (**Fig. 11b**). On the other hand, we observed a medium abundance of VGLUT2 fibers in the MSDB region. Therefore, the present study concentrated only on the VGLUT2 innervation of parvalbumin neurons.

In intact rats, the VGLUT2-containing neuronal elements appeared as varicosities ranging from 0.5-1.2 μm in diameter. The intervaricose segments of axons were only occasionally stained and very short in length. The overall distribution of VGLUT2-positive varicosities was not homogeneous in the MSDB. They gathered mainly in the medial septum/lateral septum border zone (**Fig. 8a**) and along the boundaries of the vertical limb of the diagonal band. Along the midline, relatively fewer boutons were observed. Parvalbumin-containing neurons were dispersed in this rich network of VGLUT2-IR axons and several close associations were observed both with cell bodies (**Fig. 8b-d**) and dendrites (**Fig. 8d**). In some cases, parvalbumin-positive cell bodies were completely surrounded by VGLUT2-containing varicosities (**Fig. 8b-c**) that resembled pericellular baskets.

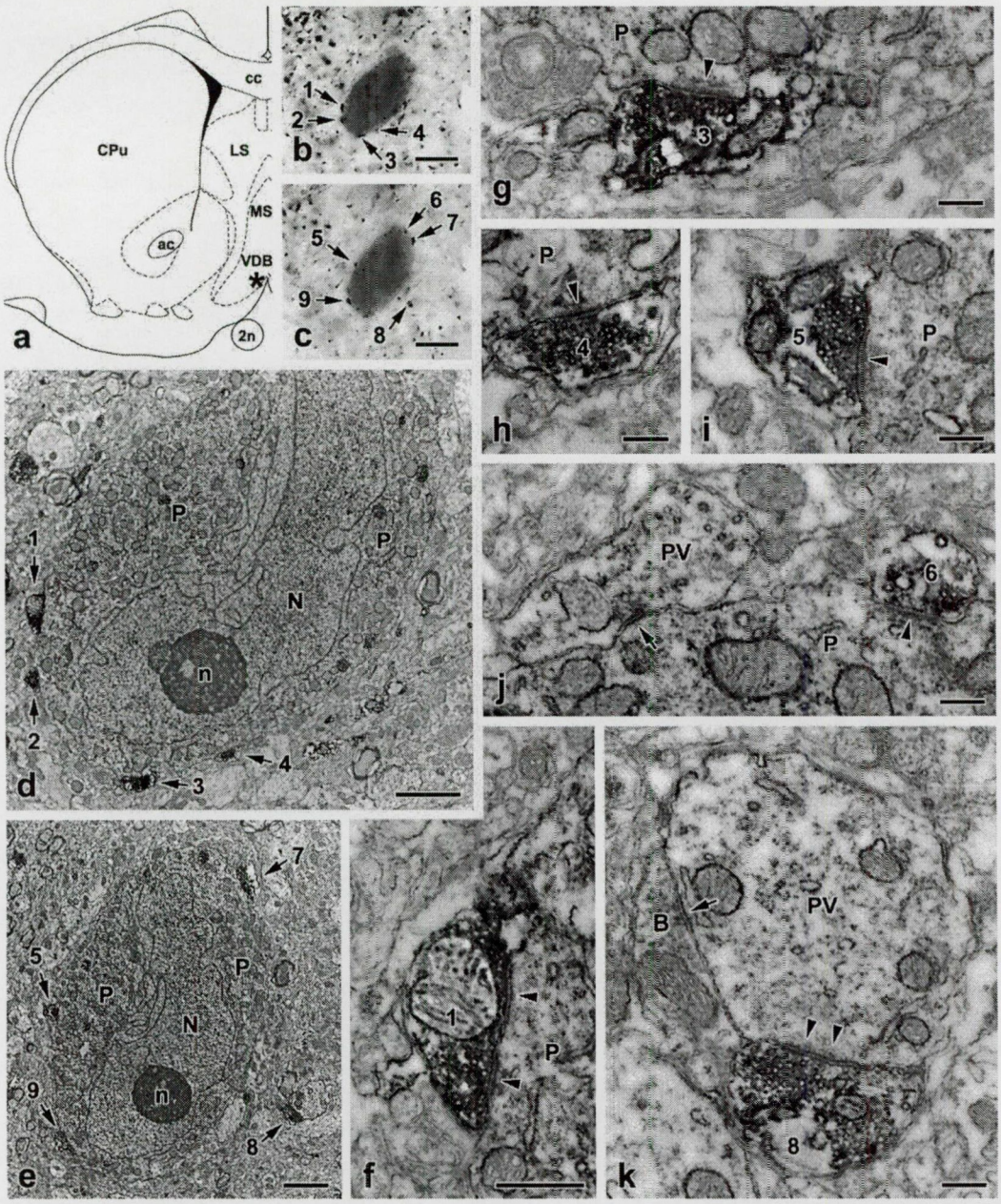

Fig. 9. Ultrastructural evidence for the existence of asymmetric, axo-somatic synaptic contacts between vesicular glutamate transporter 2 (VGLUT2)-immunoreactive varicosities and parvalbumin (PV)-positive septo-hippocampal neurons. a: In this schematic drawing, the asterisk indicates the location of the analyzed PV cell body. **b, c:** High power light micrographs showing the PV cell body at two different levels. Scale bars: 10 μm. **d, e:** These low power electron micrographs are correlated to the light micrographs of panels **b** and **c**, respectively. The numbering of VGLUT2-containing boutons in all electron micrographs refers to the numbers on panels **b** and **c**. Scale bars: 2 μm. **f-j:** High power electron micrographs demonstrate axo-somatic asymmetric synapses (arrowheads) between VGLUT2-positive boutons (1, 3, 4, 5, 6) and the PV perikaryon (P). On panel **j**, a PV-positive varicosity (PV) establishes a symmetric synapse (arrow) in the vicinity of the asymmetric synapse (arrowhead) formed by the VGLUT2-immunoreactive bouton (6). Scale bars: 250 nm. **k:** The VGLUT2-containing varicosity (8) establishes an asymmetric synapse (arrowheads) with a PV-positive dendrite (PV). In the vicinity of this synaptic contact, there is a symmetric synapse (arrow) on the same dendrite formed by an immunonegative bouton (B). Scale bar: 250 nm. **Abbreviations:** 2n: optic nerve; ac: anterior commissure; cc: corpus callosum; CPu: caudate putamen; LS: lateral septum; MS: medial septum; n: nucleolus; N: nucleus; P: PV-positive perikaryon; VDB: vertical diagonal band.

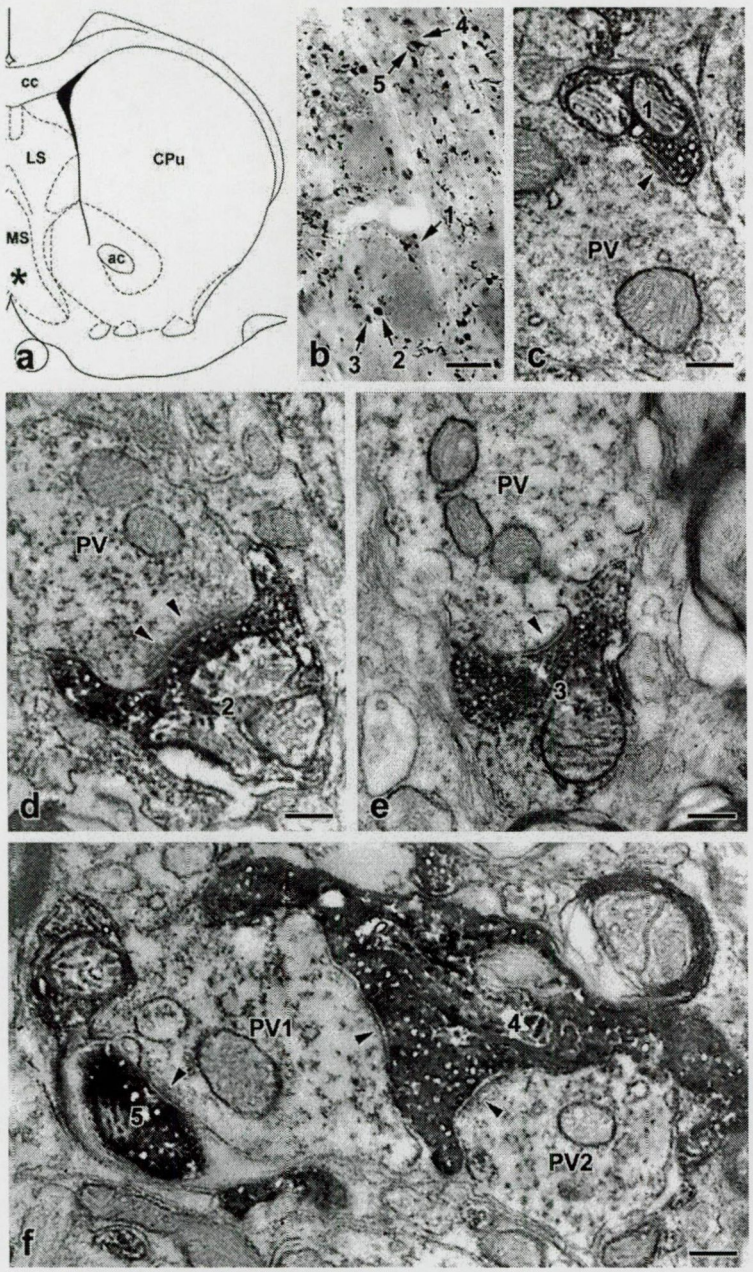

Fig. 10. Ultrastructural demonstration of asymmetric, axo-dendritic synaptic contacts between vesicular glutamate transporter 2 (VGLUT2)-immunoreactive varicosities and parvalbumin (PV)-positive dendrites. a: In this schematic drawing, the asterisk indicates the location of the analyzed tissue sample. **b:** In this high power light micrograph, the numbers label VGLUT2-immunoreactive boutons that are shown on the electron micrograph panels **c-f**. Scale bar: 10 μm. **c-f:** High power electron micrographs showing axo-dendritic asymmetric synapses (arrowheads) between VGLUT2-containing boutons (1, 2, 3, 4, 5) and PV-positive dendrites (PV). On panel **f**, the large VGLUT2-positive bouton (4) establishes asymmetric synapses with two different PV-positive dendrites (PV1 and PV2). Scale bars: 250 nm. **Abbreviations:** ac – anterior commissure; cc – corpus callosum; CPu – caudate putamen; LS – lateral septum; MS – medial septum.

The notion of strong glutamatergic influence upon septo-hippocampal GABA neurons was further strengthened by the electron microscopic observations. A total number of 24 VGLUT2/parvalbumin close associations were analyzed both in intact and SX animals. Ten of the 13 VGLUT2-IR boutons closely associated to parvalbumin cell bodies (**Fig. 9**) were revealed to establish synaptic contacts. Furthermore, of the 11 VGLUT2/parvalbumin axo-dendritic close associations, eight were found to form synapses (**Fig. 10**). All synapses were of the asymmetric type with prominent postsynaptic densities suggesting that the VGLUT2 input exerts an excitatory influence (Kandel and Siegelbaum, 2000) upon parvalbumin neurons. Occasionally, symmetric synaptic specializations were also found in the vicinity of these asymmetric synapses. The presynaptic boutons forming these symmetric synapses were either parvalbumin-positive (**Fig. 9j**) or immunonegative (**Fig. 9k**).

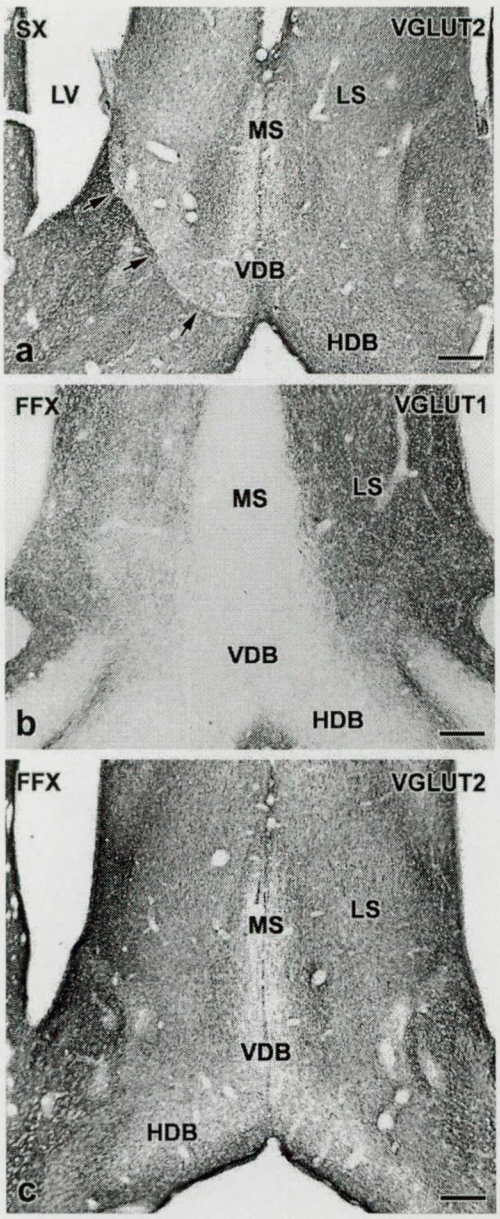

Fig. 11. Demonstration of vesicular glutamate transporter 1 and 2 (VGLUT1 and VGLUT2)-immunoreactive varicosities in the septal complex following septal deafferentations. a: This low power light micrograph shows VGLUT2 immunolabeling five days following a unilateral septal undercut (SX; arrows point to the line of lesion). Although there is an abrupt decrease in the density of VGLUT2-containing boutons in the lateral septal area (LS) ipsilateral to the lesion, there is no obvious change in the medial septal complex (MS, VDB). Abbreviations: HDB – horizontal diagonal band; LV – lateral ventricle; VDB – vertical diagonal band. Scale bar: 250 μm. **b:** Five days following fimbria/fornix transection (FFX), there is a clear decrease in VGLUT1 immunoreactivity in the LS ipsilateral to the lesion (left side on the picture). Scale bar: 250 μm. **c:** The VGLUT2 immunostaining five days after FFX demonstrates no discernible change in any septal area. The side ipsilateral to the lesion is on the left side of the picture. Scale bar: 250 μm.

The majority of VGLUT2-containing varicosities in the MSDB remains intact following septal deafferentation

Relative changes in VGLUT bouton densities. Five days following SX, no visible changes in VGLUT2 immunolabeling within the MSDB were revealed while an obvious decrease in the density of VGLUT2-positive boutons was observed in the lateral septum ipsilateral to the lesion (**Fig. 11a**). On the other hand, fimbria/fornix transection, i.e., the surgical separation of the MSDB from all afferents coming from the hippocampus via the right fimbria/fornix, caused a clear-cut decrease in VGLUT1 bouton density in the lateral septum ipsilateral to the lesion (**Fig. 11b**) demonstrating the effectiveness of the intervention. However, FFX failed to induce any visible changes in VGLUT2 immunostaining in any areas of the septum, including the MSDB (**Fig. 11c**). Despite the lack of recognizable changes under the light microscope, the quantitative analysis of the density of VGLUT2-containing boutons in the MSDB revealed significant alterations. Comparing the density values of VGLUT2-IR boutons between the ipsi- and contralateral MS/LS, there were significant ($p<0.01$) decreases in the ipsilateral side both in SX and FFX animals by 24% and 12%, respectively (**Fig. 12**). Taking into account the possibility that VGLUT2-positive axons may cross over, the density data from SX and FFX animals were compared to those from intact rats. In this paradigm, SX resulted in a

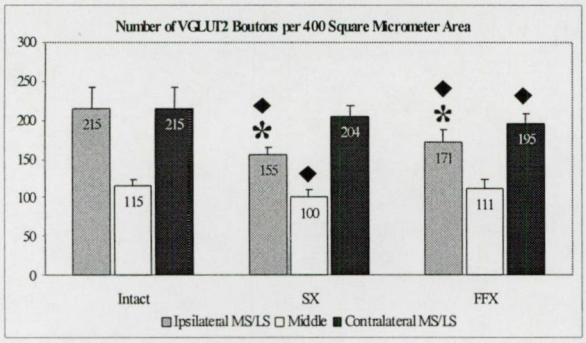

Fig. 12. Quantitative analysis of changes in the density values of vesicular glutamate transporter 2 (VGLUT2)-containing boutons in the septal complex following deafferentations. This diagram shows the number of VGLUT2-positive varicosities in a unit area in intact rats and following unilateral septal undercut (SX) and fimbria/fornix transection (FFX). Compared to the contralateral side, there was a significant decrease ($p<0.01$; asterisks) in the density of VGLUT2-containing boutons in the medial septum/lateral septum border zone (MS/LS) on the side ipsilateral to the lesion, in both the SX and FFX animals. Compared to intact animals, the bouton density was significantly decreased ($p<0.01$; diamonds) in the ipsilateral MS/LS and the middle septal area following SX, and in both the ipsi- and contralateral MS/LS following FFX ($p<0.05$). Both the contralateral MS/LS in SX animals and the middle septal area in FFX rats remained statistically unchanged following these surgical interventions.

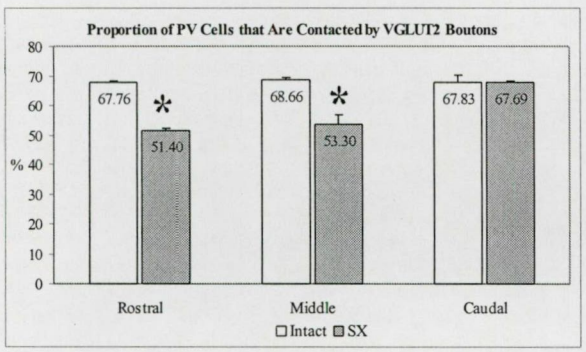

Fig. 13. Quantitative analysis of changes in the percentage of parvalbumin (PV) cells that were contacted by vesicular glutamate transporter 2 (VGLUT2)-positive boutons following septal undercut (SX). This diagram represents PV neurons that were contacted by VGLUT2-containing varicosities on their perikarya and/or proximal dendrites as percentages of all PV cells at rostral, middle, and caudal levels (see methods for Bregma values) of the medial septum diagonal band complex (MSDB), in intact and SX rats. In intact animals, the cell bodies and/or proximal dendrites of about 68% of PV neurons were contacted by VGLUT2-containing boutons at all oro-caudal levels of the MSDB. Following SX, this proportion decreased significantly (asterisks) by about 22-24% at rostral and middle levels. In contrast, there was no change in caudal regions of the MSDB.

significant ($p<0.01$) decrease in the density of VGLUT2-containing boutons of the ipsilateral MS/LS and of the middle area of the MSDB by 28% and 13%, respectively (**Fig. 12**). Following FFX, a significant ($p<0.05$) decrease in the density of VGLUT2-IR boutons was observed in both the ipsi- (21%) and contralateral (10%) MS/LS (**Fig. 12**).

Changes in VGLUT2 input to parvalbumin-positive neurons in the MSDB. The quantitative light microscopic analysis also showed alterations in the innervation of MSDB parvalbumin-positive cells by VGLUT2-containing axons, following SX. In intact animals, about 68% of parvalbumin neurons were found to be contacted by at least one VGLUT2-containing bouton on their perikarya and/or proximal dendrites, at all three levels of the MSDB (**Fig. 13**). In SX rats, this percentage decreased significantly ($p<0.01$) by 24% at the rostral level of the MSDB and by 22% at the middle level (**Fig. 13**). The SX caused no change in this percentage at the caudal level (**Fig. 13**).

Control. To determine the effective survival time after deafferentation surgeries, we performed similar VGLUT2 bouton density calculations following ten days of survival. The results were compared to data obtained from animals with five-day survival period as described above. No significant difference was observed between the two groups

(data not shown) suggesting that five-day survival is sufficient to abolish the VGLUT2 immunoreactivity of disrupted fibers.

VGLUT2-immunoreactive neurons exist in the septum

Light microscopic observation of the septum of colchicine-treated rats revealed a large number of VGLUT2-IR cell bodies distributed throughout the septal complex. In the MSDB, scattered fusiform cells were observed with their longitudinal axis parallel to the sagittal plane (**Fig. 14b**). The majority of these cells occupied mainly the MS/LS and relatively few were seen along the midline (**Fig. 14a**). In the lateral septum, small numbers of VGLUT2-positive, fusiform cell bodies were encountered, mainly in the dorsal and intermediate lateral septal nuclei (**Fig. 14a**) located at the more rostral level of the septum. On the other hand, a very dense population of VGLUT2-containing neurons was found in the caudal part of the septal complex (**Fig. 14c**). Along the midline and within the fiber bundles of the fornix, these fusiform cells were oriented parallel to the fiber bundles (**Fig. 14c**). In the septofimbrial and triangular nuclei, as well as in the caudal end of the lateral septal division, a large number of VGLUT2-IR perikarya gathered to form clusters and bundles of cell bodies (**Fig. 14d**). These clusters contained round and fusiform cells with no clear orientation of the dendritic tree. The diameter of all of these VGLUT2-containing cell bodies was found to be 10-15 μm.

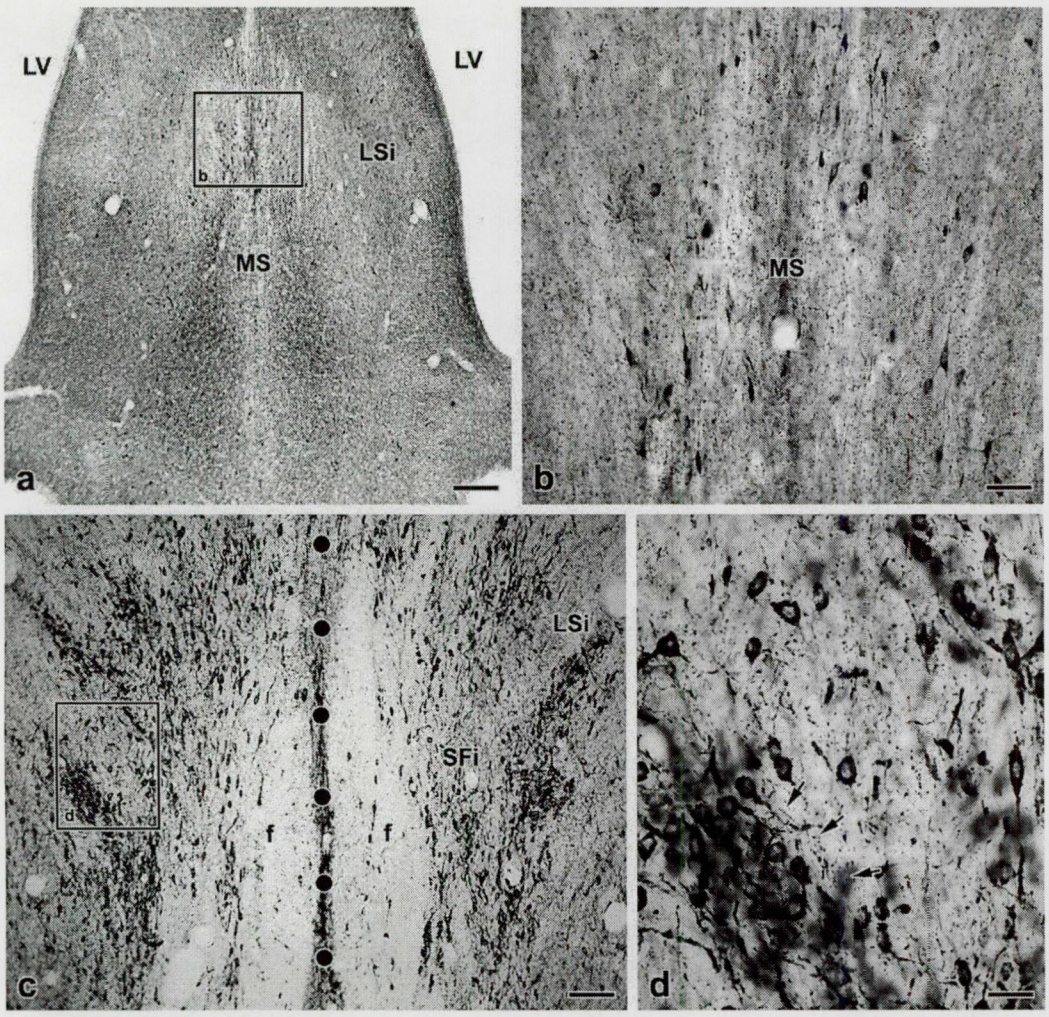

Fig. 14. Evidence for the existence of vesicular glutamate transporter 2 (VGLUT2)-immunoreactive cell bodies in the septum and their pattern of distribution. a: Taken from rostral septal areas, this low power light micrograph demonstrates VGLUT2-containing cell bodies that are located mostly in the medial septum/lateral septum border zone. Abbreviations: LSi – intermediate lateral septal nucleus; LV – lateral ventricle; MS – medial septum. Scale bar: 250 μm. **b:** Higher power micrograph of the boxed area in panel **a** shows scattered VGLUT2-immunoreactive cells in the MS. Scale bar: 50 μm. **c:** In caudal septal areas, a very rich VGLUT2-containing cell population occupies mainly the septofimbrial nucleus (SFi) and the lateral septum (LSi). Abbreviation: f – fornix. Scale bar: 100 μm. **d:** High power micrograph of the boxed area on panel **c** demonstrates a cluster of VGLUT2-containing neurons (arrows). Scale bar: 25 μm.

DISCUSSION

The adrenergic/cholinergic link in the basal forebrain

Adrenergic versus noradrenergic input to BF cholinergic neurons

In previous studies, the immunohistochemical identification of dopamine β-hydroxylase (DBH) has been used to describe noradrenergic input to the BF (Chang and Kuo, 1989; Zaborszky et al., 1993; Zaborszky and Cullinan, 1996; Milner and Prince, 1998; Rodrigo et al., 1998; Smiley and Mesulam, 1999). However, DBH-positive neuronal elements comprise *both* noradrenergic and adrenergic structures (Hökfelt et al., 1984) that renders DBH an imperfect marker for noradrenergic terminals. On the other hand, PNMT-immunoreactivity solely represents adrenergic neuronal structures. Since the central adrenergic and noradrenergic systems participate in different, and to some extent, the same functional processes, it is important to know what proportion of DBH/ChAT interaction sites does represent real noradrenergic input. By comparing the results of the present experiment (**Fig. 4**) with data obtained from the previous study on the noradrenergic innervation of BF cholinergic neurons (Zaborszky and Cullinan, 1996), it becomes obvious that noradrenergic innervation more than likely predominates in the septal complex and ventral pallidum, since these territories are almost completely devoid of PNMT/ChAT appositions, while notable amount of DBH/ChAT interactions does exist. Regarding the HDB, globus pallidus, BST, and substantia innominata, the comparison of the number of PNMT/ChAT interaction sites with that of DBH/ChAT appositions suggests that about 35-45% of the putative DBH/ChAT contact sites represent adrenergic input to BF cholinergic neurons.

Due to the widely accepted notion that the predominant catecholaminergic input to BF is represented by noradrenergic axons, electrophysiological studies (Fort et al., 1995; Berridge et al., 1996) have focused on the effects of noradrenaline on BF neurons. Since there is no affinity difference between adrenaline and noradrenaline for almost all adrenoceptors described to date (Bylund et al., 1994; Minneman and Esbenshade, 1994; Guarino et al., 1996), the differentiation between BF noradrenergic and adrenergic actions seems to be very challenging. On the other hand, the effects of noradrenaline may suggest possible actions of adrenaline. It has been suggested by several studies (Fort et al., 1995; Alreja and Liu, 1996;

Fort et al., 1998) that both cholinergic and noncholinergic neurons in the BF are affected by noradrenaline with possible involvement of α_1 and β adrenoceptors. In addition, it has been reported that acetylcholine release in the prefrontal cortex is inhibited by α_2 receptor activation in the BF (Acquas et al., 1998; Tellez et al., 1999).

The suggestion from functional experiments that adrenoceptors exist in BF territories has been confirmed by several histochemical studies. Neurons located in cholinergic BF areas have been shown to express mRNAs for α_{1a}, α_{1b}, α_{1d}, α_{2a}, α_{2c}, β_1 and β_2 adrenoceptors (Asanuma et al., 1991; McCune et al., 1993; Nicholas et al., 1993ab; Pieribone et al., 1994; Scheinin et al., 1994; Day et al., 1997; Domyancic and Morilak, 1997; Winzer-Serhan et al., 1997a). Furthermore, radiohistochemical ligand binding studies (Unnerstall et al., 1985; Boyajian et al., 1987; Zilles et al., 1991; King et al., 1995; Winzer-Serhan et al., 1997ab) have provided evidence for the existence of α_1, α_{1A}, α_{1B}, α_2, α_{2A} and α_{2C} adrenoceptor proteins in BF areas. By means of immunohistochemistry, further evidence has been given for the existence of α_{1B}, α_{2A}, α_{2C} and β adrenoceptors in BF (Wanaka et al., 1989; Aoki et al., 1994; Rosin et al., 1996; Talley et al., 1996; Acosta-Martinez et al., 1999). By comparing the locations of PNMT/ChAT appositions (**Fig. 4**) with the rough distribution pattern of the different adrenoceptor subtypes, it may be hypothesized that in the HDB and substantia innominata, where the number of appositions is high, the α_{1A}, α_{1B}, α_{2A} and β_1 receptors may be involved in adrenergic/cholinergic interactions. Since cholinergic neurons are intermingled in BF areas with different types of GABAergic and peptidergic interneurons and/or projection neurons (Zaborszky et al., 1999; Zaborszky and Duque, 2000), locally applied adrenergic drugs reach not only cholinergic neurons but other neuronal types as well. As a result, the knowledge of the cellular localization of adrenoceptors in the BF is of particular importance. Unfortunately, except for a preliminary study demonstrating α_{2A} receptor immunoreactivity in the cytoplasm of BF cholinergic neurons (Zaborszky et al., 1995), the cellular localization of other adrenoceptors has yet to be described.

Participation of the basal forebrain PNMT/ChAT interaction in autonomic control

The central adrenergic system has been well known for decades to be one of the key components of autonomic regulatory mechanisms. It is involved in the control of the neuroendocrine system, energy balance, body temperature homeostasis, stress, reproductive

behavior, and the regulation of the cardiovascular system (for review see e.g. Hökfelt et al., 1974; Saper, 1995). PNMT-IR neurons, primarily in the C1 group, display hypovolemia-induced Fos protein expression (Chan and Sawchenko, 1994; Ruggiero et al., 1996), suggesting that adrenergic neurons play an essential role in the pressor response and maintenance of tonic and reflex control of arterial pressure (Ciriello et al., 1986). Adrenergic axons from the medullary C1-C2 cell groups may transfer viscerosensory-related information directly or via the brainstem parabrachial relay to cholinergic neurons in the BF (Zaborszky et al., 1991; Saper, 1995). Recently, it has been shown that lesioning of the rat BF cholinergic system results in the abolition of β-carboline induced cardiovascular responses (Berntson et al., 1998), suggesting the involvement of the BF cholinergic system in autonomic regulation. Our quantitative analysis of the distribution of PNMT/ChAT appositions showed that the adrenergic input is biased towards cholinergic neurons in the substantia innominata (**Figs. 4 and 5**). This region contains the majority of cholinergic neurons that are known to project to cortical areas involved in autonomic control (Rye et al., 1984; Carlsen et al., 1985; Woolf, 1991), including the insular cortex (Saper, 1982; Ruggiero et al., 1987; Yasui et al., 1991) and medial prefrontal cortex (Neafsey, 1990). Furthermore, the BF cholinergic effects on autonomic functions may be mediated via central amygdaloid cells (Swanson and Petrovich, 1998; Pitkanen, 2000) since the amygdala and BF cholinergic neurons are in reciprocal connection (Zaborszky et al., 1984; Carlsen et al., 1985).

In addition to influencing specific cortical and amygdaloid areas, the adrenergic/cholinergic link in the BF may participate in autonomic control by modulating hypothalamic neuroendocrine and autonomic networks. Several experiments in the rat have provided evidence for cholinergic influence on osmosensitive neurons and vasopressin release in the hypothalamic paraventricular and supraoptic nuclei (Mason, 1985; Okuda et al., 1993; Shioda et al., 1997; Qadri et al., 1998; Zaninetti et al., 2000), and on body temperature and water intake regulation in the preoptic-anterior hypothalamic areas (Takahashi et al., 2001) and in the lateral hypothalamus (Puig de Parada et al., 1997). Although the source of cholinergic input to these neuroendocrine and autonomic networks remains to be elucidated, it is likely that at least a proportion of this input originates as collaterals of BF cholinergic neurons that receive PNMT innervation. For example, it has been suggested that the cholinergic input to the SON originates from a cell cluster located dorsolateral to this nucleus

(Meyer and Brownstein, 1980; Mason et al., 1983; Meeker et al., 1988; Theodosis and Mason, 1988). Indeed, cholinergic neurons in the immediate vicinity of the SON receive a particularly dense PNMT input (**Fig. 2g, 4d**).

Role of the basal forebrain PNMT/ChAT interaction in cortical activation

It has been proposed in earlier studies that the central adrenergic system may play a role in the regulation of sleep/wakefulness and arousal (Hökfelt et al., 1974). More recently, Foote and coworkers have shown (Berridge et al., 1996; Berridge and Foote, 1996) that β-receptor stimulation in the rostral forebrain elicits robust activation of both cortical and hippocampal EEG in rats. Atropine pretreatment was sufficient to abolish this EEG activation, indicating that it is mediated via muscarinic cholinergic mechanisms. The region of effective injection sites in the BF encompassed several structures, including the medial septum, the shell of the nucleus accumbens, ventral pallidum and the rostral part of the substantia innominata. These areas contain β-receptors, DBH/ChAT and also PNMT/ChAT appositions, suggesting that the central adrenergic system may participate in this β-receptor elicited increase in cortical activity. On the other hand, infusion of isoproterenol, a β-receptor agonist into the substantia innominata, an area that is heavily innervated by PNMT-IR fibers, failed to evoke any changes in cortical EEG (Berridge et al., 1996). In another study, however, it has been reported that infusion of noradrenaline into the substantia innominata facilitates γ-EEG activity and elicits waking (Cape and Jones, 1998). This, together with previous electrophysiological results from guinea pig BF slices (Fort et al., 1995), suggests that mainly α_1 receptors mediate the arousal-enhancing effects of both noradrenaline and adrenaline in the substantia innominata. These physiological data are in line with our results to suggest that the central adrenergic system can support cortical activation via α_1 and β adrenoceptors located on cholinergic corticopetal neurons in the BF.

Glutamate in the septo-hippocampal system

Role of glutamate in synaptic integration on septo-hippocampal GABA cells

The activity of a single neuron, i.e., triggering an action potential or remaining silent, is a consequence of the cumulative actions of all synaptic signals that reach the cell. However,

the synaptic integration does not mean the simple summation of inhibitory and excitatory inputs. If a synapse resides closer to the action potential trigger zone, i.e., near to the axon hillock, it has a larger influence on the activity of the neuron. These 'strategic' areas are the cell body, proximal dendrites, and the axon hillock. According to current knowledge, these strategic areas are overwhelmingly occupied by GABAergic inhibitory synapses while the excitatory axons synapse on dendrites and spines. Thus, the activity of the neuron is usually at the mercy of the axo-somatic inhibitory input (for review see e.g. Kandel and Siegelbaum, 2000).

In the case of septo-hippocampal GABA cells, previous studies have demonstrated a strong axo-somatic inhibitory control (Toth et al., 1993). Arising from hippocampal non-pyramidal cells, GABAergic fibers preferentially terminate on the parvalbumin neurons of the MSDB, frequently forming pericellular baskets as well as multisynaptic contacts on their dendrites. This GABAergic innervation pattern highly parallels that of the glutamatergic innervation found in the present study. Furthermore, we frequently observed the presence of symmetric (usually unlabeled) and asymmetric (VGLUT2-positive) synaptic contacts on parvalbumin-positive dendrites or cell bodies close to each other (**Fig. 9j-k**). This morphological situation may lead to the following functional consequences: (1) since glutamatergic excitatory synapses also occupy the 'strategic' areas (see above), the glutamatergic input may be capable of strongly activating the septo-hippocampal GABA cells and, in turn, hippocampal theta rhythm and cognitive functions. Physiological evidence that support this hypothesis is discussed below. (2) The distribution patterns of GABAergic and glutamatergic synapses on septo-hippocampal GABA cells, especially those located on their somata seem to be very similar. As a result, the glutamatergic excitatory input may be capable of challenging the action of the neighboring GABAergic inhibitory synapses. Thus, instead of being highly influenced by the GABAergic innervation as known to date, the activity of septo-hippocampal GABA neurons may be determined by the balanced activity of GABAergic and glutamatergic inputs.

Implications of the deafferentation experiments

In the present study, the distribution of VGLUT2-containing varicosities in the septum of intact animals was the same as published previously (Fremeau et al., 2001; Kaneko and

Fujiyama, 2002; Kaneko et al., 2002; Varoqui et al., 2002). Thus, changes in VGLUT2-positive bouton densities caused by the surgical interventions suggest that about 28% of these fibers in the MS/LS and 13% in the middle septal area have an extraseptal origin and arrive via the ventral pathway, since SX caused a VGLUT2 bouton density depletion of this magnitude. Another 31% of VGLUT2-containing boutons in the MS/LS are from axons traversing the fimbria/fornix of hippocampal origin (21% via the ipsilateral + 10% via the contralateral fimbria/fornix; data obtained from FFX animals). All of the remaining boutons, i.e., 41% in the MS/LS and 87% in the middle septal area may originate within the septum. Indeed, in colchicine-treated rats, we detected VGLUT2-immunopositive neurons throughout the septum. The distribution of these cell bodies was generally the same as previously determined by *in situ* hybridization experiments (Hisano et al., 2000; Fremeau et al., 2001; Herzog et al., 2001; Lin et al., 2003), but our results provide ultimate evidence that these neurons do express the VGLUT2 protein and they are really capable of using glutamate as neurotransmitter. Furthermore, previous studies have not shown data about the large posterior septal population of glutamatergic neurons described in the present study. Nevertheless, the exact proportional contribution of the septal VGLUT2-containing neurons to the innervation of the MSDB and septo-hippocampal GABA cells remains to be elucidated.

Functional considerations

Although several microdialysis studies have provided evidence that intraseptal infusions of different glutamatergic drugs are capable of increasing hippocampal acetylcholine outflow by as much as 500% (Giovannini et al., 1994; Moor et al., 1996; Giovannini et al., 1998; Moor et al., 1998), relatively little is known about the effect of glutamate on GABA release. It has been reported that perfusing the septum with an N-methyl-D-aspartate (NMDA)-receptor antagonist results in a decreased septal GABA outflow (Giovannini et al., 1994) suggesting a tonic glutamatergic activation of septal GABA neurons. Furthermore, intraseptal infusions of glutamate, NMDA and alpha-amino-3-hydroxy-5-methyl-4-isoxazoleproprionate (AMPA) increased hippocampal theta frequency (Puma et al., 1996; Puma and Bizot, 1999; Carre and Harley, 2000), while infusion of an NMDA-receptor antagonist caused an opposite effect (Puma et al., 1996). Since septo-hippocampal cholinergic neurons regulate primarily theta amplitude (Lee et al., 1994), changes in theta frequency

elicited by intraseptal administration of glutamatergic agents are probably mediated by septo-hippocampal GABA neurons. In behaving animals tested in different memory tasks, several authors have reported that memory processes and long-term potentiation are blocked at the time of their initiation by intraseptal infusions of both NMDA- and metabotropic glutamate-receptor antagonists (e.g., Izquierdo et al., 1992; 1993; Izquierdo, 1994; Flood et al., 1998), while infusion of glutamate causes memory facilitation. Although several types of glutamate receptors have been implicated in these experiments, only AMPA receptor proteins have been colocalized with parvalbumin in the MSDB (Martin et al., 1993; Kumamoto, 1997). All of these experiments lend support to the view that the glutamatergic influence upon septo-hippocampal GABA neurons may be a crucial and powerful driver of theta rhythm and hippocampus-associated memory processes. Our present data provide a morphological explanation for these strong glutamatergic effects.

To date, glutamatergic excitatory neurons of the central nervous system have been considered as projection cells. On the other hand, our results support the possibility that they may function as local circuit neurons, as well, and raise a new functional aspect of the extensive glutamatergic neuronal network in the brain. Recently, using electrophysiological recordings in a rat brain slice preparation, we discovered that rapid applications of nicotine excited 90% of retrogradely labeled septo-hippocampal GABA-type neurons and increased the frequency of spontaneously occurring fast GABAergic and glutamatergic synaptic currents via the $\alpha 4\beta 2$-nicotinic receptor. Interestingly, tetrodotoxin blocked all effects of nicotine on septo-hippocampal GABAergic neurons, suggesting involvement of indirect mechanisms. We demonstrated that these effects of nicotine involve the recruitment of a novel, local glutamatergic circuitry as (1) group I metabotropic glutamatergic receptor antagonists reduced the effects of nicotine; (2) the number of nicotine-responsive neurons was significantly reduced in recordings from slices that had been trimmed so as to reduce the number of glutamate-containing neurons within the slice preparation. These findings coupled with the knowledge of strong local glutamatergic input to septo-hippocampal GABA cells reveals intraseptal glutamatergic neurons as new members of the local information processing circuitry in the MSDB. As we noted above, this glutamatergic excitatory influence on the activity of septo-hippocampal parvalbumin-IR neurons seems to be as powerful as the action of its GABAergic inhibitory counterpart.

Conclusions

In the first experiment, we provided morphological evidence that adrenergic terminals synapse on cholinergic neurons of the BF. This innervation is most pronounced in the substantia innominata, that is the source of cholinergic input to a distributed forebrain network, including the prefrontal and insular cortices, the amygdala, and several hypothalamic sites involved in neuroendocrine and autonomic regulation. Cholinergic neurons together with other local and projection cells in the BF are well positioned anatomically to integrate and coordinate cognitive functions with autonomic regulation. The adrenergic input from the brainstem can provide viscerosensory, peripheral feedback to this process.

The main findings of the second experiment are: (1) VGLUT2-IR varicosities form asymmetric synaptic contacts with parvalbumin-IR cell bodies and dendrites in the MSDB. (2) A surprisingly large number of these synapses represent axo-somatic contacts. (3) Following the disruption of septal afferents, the majority of both VGLUT2-containing boutons and their synaptic contacts with parvalbumin-positive cells remained intact in the MSDB. (4) A large population of VGLUT2 protein-containing neurons exists in almost all areas of the septum. The latter two observations suggest that the major portion of MSDB glutamate axons have an intraseptal origin and raise a novel functional aspect of glutamatergic cells as local circuit neurons. A constant impulse flow in the septo-hippocampal GABA pathway is essential for the generation of theta rhythm. Thus, the heavy glutamatergic innervation of these septo-hippocampal GABA cells establishes the morphological basis for the powerful glutamatergic influence upon theta rhythm and hippocampus-associated memory processes.

ACKNOWLEDGMENTS

I dedicate this work to my wife, Dr. Nermin Samir Sallam, my parents, Márta Major and Tibor Hajszán, as well as my mentors, Prof. Csaba Léránth, Prof. Zsolt Liposits, Prof. Árpád Párducz, and Prof. László Záborszky. Having their support, patience, and guidance brought the highest value to my life.

REFERENCES

Acosta-Martinez M, Fiber JM, Brown RD, Etgen AM. 1999. Localization of alpha1B-adrenergic receptor in female rat brain regions involved in stress and neuroendocrine function. Neurochem Int 35:383-391.

Acquas E, Wilson C, Fibiger HC. 1998. Pharmacology of sensory stimulation-evoked increases in frontal cortical acetylcholine release. Neuroscience 85:73-83.

Aihara Y, Mashima H, Onda H, Hisano S, Kasuya H, Hori T, Yamada S, Tomura H, Yamada Y, Inoue I, Kojima I, Takeda J. 2000. Molecular cloning of a novel brain-type Na(+)-dependent inorganic phosphate cotransporter. J Neurochem 74:2622-2625.

Alreja M, Liu W. 1996. Noradrenaline induces IPSCs in rat medial septal/diagonal band neurons: involvement of septohippocampal GABAergic neurons. J Physiol (Lond) 494:201-215.

Alreja M, Wu M, Liu W, Atkins JB, Leranth C, Shanabrough M. 2000. Muscarinic tone sustains impulse flow in the septohippocampal GABA but not cholinergic pathway: implications for learning and memory. J Neurosci 20:8103-8110.

Aoki C, Go CG, Venkatesan C, Kurose H. 1994. Perikaryal and synaptic localization of alpha 2A-adrenergic receptor- like immunoreactivity. Brain Res 650:181-204.

Arendt T, Bruckner MK, Bigl V, Marcova L. 1995. Dendritic reorganisation in the basal forebrain under degenerative conditions and its defects in Alzheimer's disease. III. The basal forebrain compared with other subcortical areas. J Comp Neurol 351:223-246.

Armstrong DM, Ross CA, Pickel VM, Joh TH, Reis DJ. 1982. Distribution of dopamine-, noradrenaline-, and adrenaline-containing cell bodies in the rat medulla oblongata: demonstrated by the immunocytochemical localization of catecholamine biosynthetic enzymes. J Comp Neurol 212:173-187.

Asanuma M, Ogawa N, Mizukawa K, Haba K, Hirata H, Mori A. 1991. Distribution of the beta-2 adrenergic receptor messenger RNA in the rat brain by in situ hybridization histochemistry: effects of chronic reserpine treatment. Neurochem Res 16:1253-1256.

Bellocchio EE, Reimer RJ, Fremeau RT, Edwards RH. 2000. Uptake of glutamate into synaptic vesicles by an inorganic phosphate transporter. Science 289:957-960.

Berntson GG, Sarter M, Cacioppo JT. 1998. Anxiety and cardiovascular reactivity: the basal forebrain cholinergic link. Behav Brain Res 94:225-248.

Berridge CW, Bolen SJ, Manley MS, Foote SL. 1996. Modulation of forebrain electroencephalographic activity in halothane- anesthetized rat via actions of noradrenergic beta-receptors within the medial septal region. J Neurosci 16:7010-7020.

Berridge CW, Foote SL. 1996. Enhancement of behavioral and electroencephalographic indices of waking following stimulation of noradrenergic beta-receptors within the medial septal region of the basal forebrain. J Neurosci 16:6999-7009.

Bohn MC, Dreyfus CF, Friedman WJ, Markey KA. 1987. Glucocorticoid effects on phenylethanolamine N-methyltransferase (PNMT) in explants of embryonic rat medulla oblongata. Brain Res 465:257-266.

Bokor H, Csaki A, Kocsis K, Kiss J. 2002. Cellular architecture of the nucleus reuniens thalami and its putative aspartatergic/glutamatergic projection to the hippocampus and medial septum in the rat. Eur J Neurosci 16:1227-1239.

Boyajian CL, Loughlin SE, Leslie FM. 1987. Anatomical evidence for alpha-2 adrenoceptor heterogeneity: differential autoradiographic distributions of [3H]rauwolscine and [3H]idazoxan in rat brain. J Pharmacol Exp Ther 241:1079-1091.

Bylund DB, Eikenberg DC, Hieble JP, Langer SZ, Lefkowitz RJ, Minneman KP, Molinoff PB, Ruffolo RR, Trendelenburg U. 1994. International Union of Pharmacology nomenclature of adrenoceptors. Pharmacol Rev 46:121-136.

Cape EG, Jones BE. 1998. Differential modulation of high-frequency gamma-electroencephalogram activity and sleep-wake state by noradrenaline and serotonin microinjections into the region of cholinergic basalis neurons. J Neurosci 18:2653-2666.

Carlsen J, Zaborszky L, Heimer L. 1985. Cholinergic projections from the basal forebrain to the basolateral amygdaloid complex: a combined retrograde fluorescent and immunohistochemical study. J Comp Neurol 234:155-167.

Carlton SM, Honda CN, Willcockson WS, Lacrampe M, Zhang D, Denoroy L, Chung JM, Willis WD. 1991. Descending adrenergic input to the primate spinal cord and its possible role in modulation of spinothalamic cells. Brain Res 543:77-90.

Carre GP, Harley CW. 2000. Glutamatergic activation of the medial septum complex: an enhancement of the dentate gyrus population spike and accompanying EEG and unit changes. Brain Res 861:16-25.

Chan RK, Sawchenko PE. 1994. Spatially and temporally differentiated patterns of c-fos expression in brainstem catecholaminergic cell groups induced by cardiovascular challenges in the rat. J Comp Neurol 348:433-460.

Chang HT, Kuo H. 1989. Adrenergic innervation of the substantia innominata: co-localization of phenylethanolamine N-methyltransferase and tyrosine hydroxylase immunoreactivities within the same axons. Brain Res 503:350-353.

Ciriello J, Caverson MM, Polosa C. 1986. Function of the ventrolateral medulla in the control of the circulation. Brain Res 396:359-391.

Day HE, Campeau S, Watson SJ, Jr., Akil H. 1997. Distribution of alpha 1a-, alpha 1b- and alpha 1d-adrenergic receptor mRNA in the rat brain and spinal cord. J Chem Neuroanat 13:115-139.

Detari L, Rasmusson DD, Semba K. 1999. The role of basal forebrain neurons in tonic and phasic activation of the cerebral cortex. Prog Neurobiol 58:249-277.

Domyancic AV, Morilak DA. 1997. Distribution of alpha1A adrenergic receptor mRNA in the rat brain visualized by in situ hybridization. J Comp Neurol 386:358-378.

Dringenberg HC. 2000. Alzheimer's disease: more than a 'cholinergic disorder' - evidence that cholinergic-monoaminergic interactions contribute to EEG slowing and dementia. Behav Brain Res 115:235-249.

Everitt BJ, Robbins TW. 1997. Central cholinergic systems and cognition. Annu Rev Psychol 48:649-684.

Flood JF, Farr SA, Uezu K, Morley JE. 1998. The pharmacology of post-trial memory processing in septum. Eur J Pharmacol 350:31-38.

Fort P, Khateb A, Pegna A, Muhlethaler M, Jones BE. 1995. Noradrenergic modulation of cholinergic nucleus basalis neurons demonstrated by in vitro pharmacological and immunohistochemical evidence in the guinea-pig brain. Eur J Neurosci 7:1502-1511.

Fort P, Khateb A, Serafin M, Muhlethaler M, Jones BE. 1998. Pharmacological characterization and differentiation of non-cholinergic nucleus basalis neurons in vitro. Neuroreport 9:61-65.

Fremeau RT, Troyer MD, Pahner I, Nygaard GO, Tran CH, Reimer RJ, Bellocchio EE, Fortin D, Storm-Mathisen J, Edwards RH. 2001. The expression of vesicular glutamate transporters defines two classes of excitatory synapse. Neuron 31:247-260.

Freund TF. 1989. GABAergic septohippocampal neurons contain parvalbumin. Brain Res 478:375-381.

Freund TF, Antal M. 1988. GABA-containing neurons in the septum control inhibitory interneurons in the hippocampus. Nature 336:170-173.

Frotscher M, Leranth C. 1985. Cholinergic innervation of the rat hippocampus as revealed by choline acetyltransferase immunocytochemistry: a combined light and electron microscopic study. J Comp Neurol 239:237-246.

Gaykema RP, Zaborszky L. 1996. Direct catecholaminergic-cholinergic interactions in the basal forebrain. II. Substantia nigra-ventral tegmental area projections to cholinergic neurons. J Comp Neurol 374:555-577.

Giovannini MG, Mutolo D, Bianchi L, Michelassi A, Pepeu G. 1994. NMDA receptor antagonists decrease GABA outflow from the septum and increase acetylcholine outflow from the hippocampus: a microdialysis study. J Neurosci 14:1358-1365.

Giovannini MG, Rakovska A, Della Corte L, Bianchi L, Pepeu G. 1998. Activation of non-NMDA receptors stimulates acetylcholine and GABA release from dorsal hippocampus: a microdialysis study in the rat. Neurosci Lett 243:152-156.

Gonzalo-Ruiz A, Morte L. 2000. Localization of amino acids, neuropeptides and cholinergic markers in neurons of the septum-diagonal band complex projecting to the retrosplenial granular cortex of the rat. Brain Res Bull 52:499-510.

Guarino RD, Perez DM, Piascik MT. 1996. Recent advances in the molecular pharmacology of the alpha 1-adrenergic receptors. Cell Signal 8:323-333.

Herzog E, Bellenchi GC, Gras C, Bernard V, Ravassard P, Bedet C, Gasnier B, Giros B, El Mestikawy S. 2001. The existence of a second vesicular glutamate transporter specifies subpopulations of glutamatergic neurons. J Neurosci 21:RC181.

Hisano S, Hoshi K, Ikeda Y, Maruyama D, Kanemoto M, Ichijo H, Kojima I, Takeda J, Nogami H. 2000. Regional expression of a gene encoding a neuron-specific Na(+)-dependent inorganic phosphate cotransporter (DNPI) in the rat forebrain. Mol Brain Res 83:34-43.

Hobson JA, Pace-Schott EF. 2002. The cognitive neuroscience of sleep: neuronal systems, consciousness and learning. Nat Rev Neurosci 3:679-693.

Hökfelt T, Fuxe K, Goldstein M, Johansson O. 1974. Immunohistochemical Evidence for the Existence of Adrenaline Neurons in the Rat Brain. Brain Res 66:235-251.

Hökfelt T, Johansson O, Goldstein M. 1984. Central Catecholamine Neurons as Revealed by Immunohistochemistry with Special Reference to Adrenaline Neurons. In: Björklund A, Hökfelt T, editors. Handbook of Chemical Neuroanatomy. New York: Elsevier. p 157-276.

Izquierdo I. 1994. Pharmacological evidence for a role of long-term potentiation in memory. Faseb J 8:1139-1145.

Izquierdo I, da Cunha C, Rosat R, Jerusalinsky D, Ferreira MB, Medina JH. 1992. Neurotransmitter receptors involved in post-training memory processing by the amygdala, medial septum, and hippocampus of the rat. Behav Neural Biol 58:16-26.

Izquierdo I, Medina JH, Bianchin M, Walz R, Zanatta MS, Da Silva RC, Bueno e Silva M, Ruschel AC, Paczko N. 1993. Memory processing by the limbic system: role of specific neurotransmitter systems. Behav Brain Res 58:91-98.

Jakab RL, Leranth C. 1994. Septum. In: Paxinos G, editor. The Rat Nervous System. San Diego, New York, Boston, London, Sydney, Tokyo, Toronto: Academic Press, Inc. p 405-442.

Jaskiw GE, Tizabi Y, Lipska BK, Kolachana BS, Wyatt RJ, Gilad GM. 1991. Evidence for a frontocortical-septal glutamatergic pathway and compensatory changes in septal glutamate uptake after cortical and fornix lesions in the rat. Brain Res 550:7-10.

Jellinger K. 1990. New developments in the pathology of Parkinson's disease. In: Streifler MB, Kprcyn AD, Melamed E, Youdim MBH, editors. Advances in Neurology. New York: Raven Press. p 1-6.

Jones BE, Muhlethaler M. 1999. Cholinergic and GABAergic neurons of the basal forebrain: Role in cortical activation. In: Lydic R, Baghdoyan HA, editors. Handbook of Behavioral State Control - Cellular and Molecular Mechanisms. New York: CRC Press. p 213-234.

Kandel ER, Siegelbaum SA. 2000. Synaptic integration. In: Kandel ER, Schwartz JH, Jessell TM, editors. Principles of Neural Science, 4th ed. New York: McGraw-Hill. p 207-227.

Kaneko T, Fujiyama F. 2002. Complementary distribution of vesicular glutamate transporters in the central nervous system. Neurosci Res 42:243-250.

Kaneko T, Fujiyama F, Hioki H. 2002. Immunohistochemical localization of candidates for vesicular glutamate transporters in the rat brain. J Comp Neurol 444:39-62.

King PR, Gundlach AL, Louis WJ. 1995. Quantitative autoradiographic localization in rat brain of alpha 2- adrenergic and non-adrenergic I-receptor binding sites labelled by [3H]rilmenidine. Brain Res 675:264-278.

Kiss J, Csaki A, Bokor H, Kocsis K, Kocsis B. 2002. Possible glutamatergic/aspartatergic projections to the supramammillary nucleus and their origins in the rat studied by selective [(3)H]D-aspartate labelling and immunocytochemistry. Neuroscience 111:671-691.

Kiss J, Csaki A, Bokor H, Shanabrough M, Leranth C. 2000. The supramammillo-hippocampal and supramammillo-septal glutamatergic/aspartatergic projections in the rat: a combined [3H]D-aspartate autoradiographic and immunohistochemical study. Neuroscience 97:657-669.

Kohler C, Chan-Palay V, Wu JY. 1984. Septal neurons containing glutamic acid decarboxylase immunoreactivity project to the hippocampal region in the rat brain. Anat Embryol (Berl) 169:41-44.

Kumamoto E. 1997. The pharmacology of amino-acid responses in septal neurons. Prog Neurobiol 52:197-259.

Lee MG, Chrobak JJ, Sik A, Wiley RG, Buzsaki G. 1994. Hippocampal theta activity following selective lesion of the septal cholinergic system. Neuroscience 62:1033-1047.

Leranth C, Carpi D, Buzsaki G, Kiss J. 1999. The entorhino-septo-supramammillary nucleus connection in the rat: morphological basis of a feedback mechanism regulating hippocampal theta rhythm. Neuroscience 88:701-718.

Leranth C, Kiss J. 1996. A population of supramammillary area calretinin neurons terminating on medial septal area cholinergic and lateral septal area calbindin-containing cells are aspartate/glutamatergic. J Neurosci 16:7699-7710.

Leranth C, Shanabrough M, Horvath TL. 2000. Hormonal regulation of hippocampal spine synapse density involves subcortical mediation. Neuroscience 101:349-356.

Leranth C, Vertes RP. 1999. Median raphe serotonergic innervation of medial septum/diagonal band of Broca (MSDB) parvalbumin-containing neurons: possible involvement of the MSDB in the desynchronization of the hippocampal EEG. J Comp Neurol 410:586-598.

Lin W, McKinney K, Liu L, Lakhlani S, Jennes L. 2003. Distribution of vesicular glutamate transporter-2 messenger ribonucleic Acid and protein in the septum-hypothalamus of the rat. Endocrinology 144:662-670.

Liposits Z, Setalo G, Flerko B. 1984. Application of the silver-gold intensified 3,3'-diaminobenzidine chromogen to the light and electron microscopic detection of the luteinizing hormone-releasing hormone system of the rat brain. Neuroscience 13:513-525.

Manns ID, Mainville L, Jones BE. 2001. Evidence for glutamate, in addition to acetylcholine and GABA, neurotransmitter synthesis in basal forebrain neurons projecting to the entorhinal cortex. Neuroscience 107:249-263.

Martin LJ, Blackstone CD, Levey AI, Huganir RL, Price DL. 1993. Cellular localizations of AMPA glutamate receptors within the basal forebrain magnocellular complex of rat and monkey. J Neurosci 13:2249-2263.

Mason WT. 1985. Staining of the magnocellular nuclei of the rat hypothalamus by a monoclonal antibody directed against the alpha-subunit of the nicotinic cholinergic receptor. Neurosci Lett 59:89-95.

Mason WT, Ho YW, Eckenstein F, Hatton GI. 1983. Mapping of cholinergic neurons associated with rat supraoptic nucleus: combined immunocytochemical and histochemical identification. Brain Res Bull 11:617-626.

McCune SK, Voigt MM, Hill JM. 1993. Expression of multiple alpha adrenergic receptor subtype messenger RNAs in the adult rat brain. Neuroscience 57:143-151.

Meeker RB, Swanson DJ, Hayward JN. 1988. Local synaptic organization of cholinergic neurons in the basolateral hypothalamus. J Comp Neurol 276:157-168.

Meyer DK, Brownstein MJ. 1980. Effect of surgical deafferentation of the supraoptic nucleus on its choline acetyltransferase content. Brain Res 193:566-569.

Milner TA. 1991. Cholinergic neurons in the rat septal complex: ultrastructural characterization and synaptic relations with catecholaminergic terminals. J Comp Neurol 314:37-54.

Milner TA, Prince SR. 1998. Parvalbumin immunoreactive neurons in the rat septal complex have substantial glial coverage and receive few direct contacts from catecholaminergic terminals. J Neurosci Res 52:723-735.

Minneman KP, Esbenshade TA. 1994. Alpha 1-adrenergic receptor subtypes. Annu Rev Pharmacol Toxicol 34:117-133.

Momiyama T, Sim JA. 1996. Modulation of inhibitory transmission by dopamine in rat basal forebrain nuclei: activation of presynaptic D1-like dopaminergic receptors. J Neurosci 16:7505-7512.

Moor E, Auth F, DeBoer P, Westerink BH. 1996. Septal and hippocampal glutamate receptors modulate the output of acetylcholine in hippocampus: a microdialysis study. J Neurochem 67:310-316.

Moor E, Schirm E, Jacso J, Westerink BH. 1998. Involvement of medial septal glutamate and GABAA receptors in behaviour-induced acetylcholine release in the hippocampus: a dual probe microdialysis study. Brain Res 789:1-8.

Moruzzi G, Magoun HW. 1949. Brain stem reticular formation and activation of the EEG. Electroencephalogr Clin Neurophysiol 1:455-473.

Mufson EJ, Bothwell M, Kordower JH. 1989. Loss of nerve growth factor receptor-containing neurons in Alzheimer's disease: a quantitative analysis across subregions of the basal forebrain. Exp Neurol 105:221-232.

Muir JL. 1997. Acetylcholine, aging, and Alzheimer's disease. Pharmacol Biochem Behav 56:687-696.

Neafsey EJ. 1990. Prefrontal cortical control of the autonomic nervous system: anatomical and physiological observations. Prog Brain Res 85:147-165.

Nicholas AP, Pieribone V, Hokfelt T. 1993a. Distributions of mRNAs for alpha-2 adrenergic receptor subtypes in rat brain: an in situ hybridization study. J Comp Neurol 328:575-594.

Nicholas AP, Pieribone VA, Hokfelt T. 1993b. Cellular localization of messenger RNA for beta-1 and beta-2 adrenergic receptors in rat brain: an in situ hybridization study. Neuroscience 56:1023-1039.

Okuda H, Shioda S, Nakai Y, Nakayama H, Okamoto M, Nakashima T. 1993. Immunocytochemical localization of nicotinic acetylcholine receptor in rat hypothalamus. Brain Res 625:145-151.

Pace-Schott EF, Hobson JA. 2002. The neurobiology of sleep: genetics, cellular physiology and subcortical networks. Nat Rev Neurosci 3:591-605.

Palkovits M, Brownstein MJ. 1988. Catecholamines in the Central Nervous System. In: Handbook of Experimental Pharmacology. p 1-26.

Peterson GM, Williams LR, Varon S, Gage FH. 1987. Loss of GABAergic neurons in medial septum after fimbria-fornix transection. Neurosci Lett 76:140-144.

Phelix CF, Liposits Z, Paull WK. 1992. Monoamine innervation of bed nucleus of stria terminalis: an electron microscopic investigation. Brain Res Bull 28:949-965.

Pieribone VA, Nicholas AP, Dagerlind A, Hokfelt T. 1994. Distribution of alpha 1 adrenoceptors in rat brain revealed by in situ hybridization experiments utilizing subtype-specific probes. J Neurosci 14:4252-4268.

Pitkanen A. 2000. Connectivity of rat amygdaloid complex. In: Aggleton JP, editor. The Amygdala. A Functional Analysis, 2nd ed. Oxford: University Press. p 31-115.

Puig de Parada M, Paez X, Parada MA, Hernandez L, Molina G, Murzi E, Contreras Q. 1997. Changes in dopamine and acetylcholine release in the rat lateral hypothalamus during deprivation-induced drinking. Neurosci Lett 227:153-156.

Puma C, Bizot JC. 1999. Hippocampal theta rhythm in anesthetized rats: role of AMPA glutamate receptors. Neuroreport 10:2297-2300.

Puma C, Monmaur V, Sharif A, Monmaur P. 1996. Intraseptal infusion of selective and competitive glutamate receptor agonist NMDA and antagonist D-2-amino-5-phosphonopentanoic acid spectral implications for the physostigmine-induced hippocampal theta rhythm in urethane-anesthetized rats. Exp Brain Res 109:384-392.

Qadri F, Waldmann T, Wolf A, Hohle S, Rascher W, Unger T. 1998. Differential contribution of angiotensinergic and cholinergic receptors in the hypothalamic paraventricular nucleus to osmotically induced AVP release. J Pharmacol Exp Ther 285:1012-1018.

Rechtschaffen A, Siegel J. 2000. Sleep and dreaming. In: Kandel ER, Schwartz JH, Jessell TM, editors. Principles of Neural Science, 4th ed. New York: McGraw-Hill. p 936-947.

Rodrigo J, Fernandez P, Bentura ML, de Velasco JM, Serrano J, Uttenthal O, Martinez-Murillo R. 1998. Distribution of catecholaminergic afferent fibres in the rat globus pallidus and their relations with cholinergic neurons. J Chem Neuroanat 15:1-20.

Rosin DL, Talley EM, Lee A, Stornetta RL, Gaylinn BD, Guyenet PG, Lynch KR. 1996. Distribution of alpha 2C-adrenergic receptor-like immunoreactivity in the rat central nervous system. J Comp Neurol 372:135-165.

Ruggiero DA, Mraovitch S, Granata AR, Anwar M, Reis DJ. 1987. A role of insular cortex in cardiovascular function. J Comp Neurol 257:189-207.

Ruggiero DA, Ross CA, Anwar M, Park DH, Joh TH, Reis DJ. 1985. Distribution of neurons containing phenylethanolamine N-methyltransferase in medulla and hypothalamus of rat. J Comp Neurol 239:127-154.

Ruggiero DA, Tong S, Anwar M, Gootman N, Gootman PM. 1996. Hypotension-induced expression of the c-fos gene in the medulla oblongata of piglets. Brain Res 706:199-209.

Rye DB, Wainer BH, Mesulam MM, Mufson EJ, Saper CB. 1984. Cortical projections arising from the basal forebrain: a study of cholinergic and noncholinergic components employing combined retrograde tracing and immunohistochemical localization of choline acetyltransferase. Neuroscience 13:627-643.

Saper CB. 1982. Convergence of autonomic and limbic connections in the insular cortex of the rat. J Comp Neurol 210:163-173.

Saper CB. 1995. Central autonomic system. In: Paxinos G, editor. The Rat Nervous System, 2nd ed. San Diego: Academic Press. p 107-135.

Saper CB. 2000. Brain stem modulation of sensation, movement, and consciousness. In: Kandel ER, Schwartz JH, Jessell TM, editors. Principles of Neural Science, 4th ed. New York: McGraw-Hill. p 889-909.

Sarter M, Bruno JP. 1999. Abnormal regulation of corticopetal cholinergic neurons and impaired information processing in neuropsychiatric disorders. Trends Neurosci 22:67-74.

Sarter M, Bruno JP. 2000. Cortical cholinergic inputs mediating arousal, attentional processing and dreaming: differential afferent regulation of the basal forebrain by telencephalic and brainstem afferents. Neuroscience 95:933-952.

Scheinin M, Lomasney JW, Hayden-Hixson DM, Schambra UB, Caron MG, Lefkowitz RJ, Fremeau RT. 1994. Distribution of alpha 2-adrenergic receptor subtype gene expression in rat brain. Mol Brain Res 21:133-149.

Semba K, Reiner PB, McGeer EG, Fibiger HC. 1988. Brainstem afferents to the magnocellular basal forebrain studied by axonal transport, immunohistochemistry, and electrophysiology in the rat. J Comp Neurol 267:433-453.

Shioda S, Yada T, Muroya S, Takigawa M, Nakai Y. 1997. Nicotine increases cytosolic Ca2+ in vasopressin neurons. Neurosci Res 29:311-318.

Smiley JF, Mesulam MM. 1999. Cholinergic neurons of the nucleus basalis of Meynert receive cholinergic, catecholaminergic and GABAergic synapses: an electron microscopic investigation in the monkey. Neuroscience 88:241-255.

Smiley JF, Subramanian M, Mesulam MM. 1999. Monoaminergic-cholinergic interactions in the primate basal forebrain. Neuroscience 93:817-829.

Sutcliffe JG, de Lecea L. 2002. The hypocretins: setting the arousal threshold. Nat Rev Neurosci 3:339-349.

Swanson LW, Petrovich GD. 1998. What is the amygdala? Trends Neurosci 21:323-331.

Szeidemann Z, Jakab RL, Shanabrough M, Leranth C. 1995. Extrinsic and intrinsic substance P innervation of the rat lateral septal area calbindin cells. Neuroscience 69:1205-1221.

Takahashi A, Kishi E, Ishimaru H, Ikarashi Y, Maruyama Y. 2001. Role of preoptic and anterior hypothalamic cholinergic input on water intake and body temperature. Brain Res 889:191-199.

Takamori S, Rhee JS, Rosenmund C, Jahn R. 2000. Identification of a vesicular glutamate transporter that defines a glutamatergic phenotype in neurons. Nature 407:189-194.

Talley EM, Rosin DL, Lee A, Guyenet PG, Lynch KR. 1996. Distribution of alpha 2A-adrenergic receptor-like immunoreactivity in the rat central nervous system. J Comp Neurol 372:111-134.

Tellez S, Colpaert F, Marien M. 1999. Alpha2-adrenoceptor modulation of cortical acetylcholine release in vivo. Neuroscience 89:1041-1050.

Theodosis DT, Mason WT. 1988. Choline acetyltransferase immunocytochemical staining of the rat supraoptic nucleus and its surroundings. A light- and electron-microscopic study. Cell Tissue Res 254:119-124.

Toth K, Borhegyi Z, Freund TF. 1993. Postsynaptic targets of GABAergic hippocampal neurons in the medial septum-diagonal band of broca complex. J Neurosci 13:3712-3724.

Tucker DC, Saper CB, Ruggiero DA, Reis DJ. 1987. Organization of central adrenergic pathways: I. Relationships of ventrolateral medullary projections to the hypothalamus and spinal cord. J Comp Neurol 259:591-603.

Unnerstall JR, Fernandez I, Orensanz LM. 1985. The alpha-adrenergic receptor: radiohistochemical analysis of functional characteristics and biochemical differences. Pharmacol Biochem Behav 22:859-874.

Varoqui H, Schafer MK, Zhu H, Weihe E, Erickson JD. 2002. Identification of the differentiation-associated Na+/PI transporter as a novel vesicular glutamate transporter expressed in a distinct set of glutamatergic synapses. J Neurosci 22:142-155.

Vertes RP, Kocsis B. 1997. Brainstem-diencephalo-septohippocampal systems controlling the theta rhythm of the hippocampus. Neuroscience 81:893-926.

Wanaka A, Kiyama H, Murakami T, Matsumoto M, Kamada T, Malbon CC, Tohyama M. 1989. Immunocytochemical localization of beta-adrenergic receptors in the rat brain. Brain Res 485:125-140.

Whitehouse PJ, Price DL, Struble RG, Clark AW, Coyle JT, Delon MR. 1982. Alzheimer's disease and senile dementia: loss of neurons in the basal forebrain. Science 215:1237-1239.

Winzer-Serhan UH, Raymon HK, Broide RS, Chen Y, Leslie FM. 1997a. Expression of alpha 2 adrenoceptors during rat brain development--I. Alpha 2A messenger RNA expression. Neuroscience 76:241-260.

Winzer-Serhan UH, Raymon HK, Broide RS, Chen Y, Leslie FM. 1997b. Expression of alpha 2 adrenoceptors during rat brain development--II. Alpha 2C messenger RNA expression and [3H]rauwolscine binding. Neuroscience 76:261-272.

Woolf NJ. 1991. Cholinergic systems in mammalian brain and spinal cord. Prog Neurobiol 37:475-524.

Wu M, Shanabrough M, Leranth C, Alreja M. 2000. Cholinergic excitation of septohippocampal GABA but not cholinergic neurons: implications for learning and memory. J Neurosci 20:3900-3908.

Yasui Y, Breder CD, Saper CB, Cechetto DF. 1991. Autonomic responses and efferent pathways from the insular cortex in the rat. J Comp Neurol 303:355-374.

Zaborszky L, Cullinan WE. 1996. Direct catecholaminergic-cholinergic interactions in the basal forebrain. I. Dopamine-beta-hydroxylase- and tyrosine hydroxylase input to cholinergic neurons. J Comp Neurol 374:535-554.

Zaborszky L, Cullinan WE, Braun A. 1991. Afferents to basal forebrain cholinergic projection neurons: an update. Adv Exp Med Biol 295:43-100.

Zaborszky L, Cullinan WE, Luine VN. 1993. Catecholaminergic-cholinergic interaction in the basal forebrain. Prog Brain Res 98:31-49.

Zaborszky L, Duque A. 2000. Local synaptic connections of basal forebrain neurons. Behav Brain Res 115:143-158.

Zaborszky L, Duque A. 2003. Sleep-wake mechanisms and basal forebrain circuitry. Front Biosci 8:d1146-1169.

Zaborszky L, Kiss J, Rosin DL. 1995. Alpha2A adrenergic receptors are present in basal forebrain cholinergic projection neurons. Soc Neurosci Abstr 21:69.

Zaborszky L, Leranth C, Heimer L. 1984. Ultrastructural evidence of amygdalofugal axons terminating on cholinergic cells of the rostral forebrain. Neurosci Lett 52:219-225.

Zaborszky L, Pang K, Somogyi J, Nadasdy Z, Kallo I. 1999. The basal forebrain corticopetal system revisited. Ann NY Acad Sci 877:339-367.

Zagon A, Totterdell S, Jones RS. 1994. Direct projections from the ventrolateral medulla oblongata to the limbic forebrain: anterograde and retrograde tract-tracing studies in the rat. J Comp Neurol 340:445-468.

Zaninetti M, Blanchet C, Tribollet E, Bertrand D, Raggenbass M. 2000. Magnocellular neurons of the rat supraoptic nucleus are endowed with functional nicotinic acetylcholine receptors. Neuroscience 95:319-323.

Zilles K, Werner L, Qu M, Schleicher A, Gross G. 1991. Quantitative autoradiography of 11 different transmitter binding sites in the basal forebrain region of the rat--evidence of heterogeneity in distribution patterns. Neuroscience 42:473-481.